

Cross sections for inelastic meson-meson scattering via quark-antiquark annihilation

Zhen-Yu Shen¹, Xiao-Ming Xu¹, and H. J. Weber²

¹Department of Physics, Shanghai University, Baoshan, Shanghai 200444, China

²Department of Physics, University of Virginia, Charlottesville, VA 22904, USA

Abstract

We study inelastic meson-meson scattering that is governed by quark-antiquark annihilation and creation involving a quark and an antiquark annihilating into a gluon, and subsequently the gluon creating another quark-antiquark pair. The resultant hadronic reactions include for $I = 1$: $\pi\pi \rightarrow \rho\rho$, $K\bar{K} \rightarrow K^*\bar{K}^*$, $K\bar{K}^* \rightarrow K^*\bar{K}$, $K^*\bar{K} \rightarrow K^*\bar{K}^*$, as well as $\pi\pi \rightarrow K\bar{K}$, $\pi\rho \rightarrow K\bar{K}^*$, $\pi\rho \rightarrow K^*\bar{K}$, and $K\bar{K} \rightarrow \rho\rho$. In each reaction, one or two Feynman diagrams are involved in the Born approximation. We derive formulas for the unpolarized cross section, the transition amplitude, and the transition potential for quark-antiquark annihilation and creation. The unpolarized cross sections for the reactions are calculated at six temperatures, and prominent temperature dependence is found. It is due to differences among mesonic temperature dependence in hadronic matter.

Keywords: Inelastic meson-meson scattering, Quark-antiquark annihilation, Quark potential model.

PACS: 13.75.Lb; 12.39.Jh; 12.39.Pn

I. INTRODUCTION

All possible meson-meson scattering takes place in hadronic matter that is created in ultrarelativistic heavy-ion collisions. Yet, no hadronic meson beam collision experiments are possible. Therefore, we need to study meson-meson scattering theoretically. In

Refs. [1, 2] we have treated in the first Born approximation the quark interchange mechanism [3] in the endothermic nonresonant reactions $\pi\pi \rightarrow \rho\rho$ for $I = 2$, $KK \rightarrow K^*K^*$ for $I = 1$, $KK^* \rightarrow K^*K^*$ for $I = 1$, $\pi K \rightarrow \rho K^*$ for $I = 3/2$, $\pi K^* \rightarrow \rho K^*$ for $I = 3/2$, $\rho K \rightarrow \rho K^*$ for $I = 3/2$, and $\pi K^* \rightarrow \rho K$ for $I = 3/2$. In some regimes, these reactions are governed by quark interchange. Cross sections for these reactions change considerably with temperature of hadronic matter. For example, every reaction has a rising peak cross section when the temperature becomes critical. Clearly, meson-meson scattering in hadronic matter has interesting features that need to be studied.

Meson-meson scattering can be mediated not only by quark interchange but also by quark-antiquark annihilation and resonances. In the present work, we concentrate on meson-meson scattering that happens through quark-antiquark annihilation. Starting from an effective Lagrangian, cross sections for $\pi\pi \rightarrow K\bar{K}$, $\rho\rho \rightarrow K\bar{K}$, $\pi\rho \rightarrow K\bar{K}^*$, and $\pi\rho \rightarrow K^*\bar{K}$ in vacuum through one-meson exchange have been obtained in Ref. [4]. Many other reactions are also possible in hadronic matter. Here we consider not only the four reactions $\pi\pi \rightarrow K\bar{K}$, $K\bar{K} \rightarrow \rho\rho$, $\pi\rho \rightarrow K\bar{K}^*$, and $\pi\rho \rightarrow K^*\bar{K}$, but also $K\bar{K} \rightarrow K^*\bar{K}^*$, $K\bar{K}^* \rightarrow K^*\bar{K}^*$, $K^*\bar{K} \rightarrow K^*\bar{K}^*$, and $\pi\pi \rightarrow \rho\rho$ for $I = 1$, which are governed by quark-antiquark annihilation. These reactions are important in the evolution of hadronic matter created in ultrarelativistic heavy-ion collisions [5–7].

In the first Born approximation, we consider the annihilation of a quark-antiquark pair into a gluon and the creation of another quark-antiquark pair from the gluon. Gluon propagation has already been taken into account in $p\bar{p}$ annihilation into mesons. Different approximations to the gluon propagation have been made to derive transition potentials in Refs. [8–10]. These are the 3S_1 models. The $p\bar{p}$ annihilation into mesons has also been studied in the 3P_0 model where a quark and an antiquark annihilate into the vacuum and another quark-antiquark pair is created from the vacuum [11, 12]. This nonperturbative mechanism is not considered here.

This paper is organized as follows. In Sect. II we derive the formulas of unpolarized cross section for meson-meson reactions that are governed by the annihilation and creation of a quark-antiquark pair. In Sect. III we derive a transition potential for the annihilation

and creation of a quark-antiquark pair. In Sect. IV we present transition amplitudes and calculate color matrix elements, spin matrix elements, and flavor matrix elements. In Sect. V we provide mesonic quark-antiquark relative-motion wave functions. In Sect. VI we calculate elastic phase shifts for $\pi\pi$ scattering for $I = 0$ and $I = 1$, calculate unpolarized cross sections for nine channels of inelastic meson-meson scattering that is governed by quark-antiquark annihilation and creation, and give relevant discussions. In Sect. VII we summarize the present work.

II. CROSS-SECTION FORMULAS

If the quark q_1 of meson $A(q_1\bar{q}_1)$ has the same flavor as the antiquark \bar{q}_2 of meson $B(q_2\bar{q}_2)$ and/or the antiquark \bar{q}_1 and the quark q_2 have the same flavor, the reaction $A + B \rightarrow C + D$ may take place through quark-antiquark annihilation and creation as shown in Fig. 1. Corresponding to the two Feynman diagrams, the S -matrix element for $A + B \rightarrow C + D$ is

$$S_{fi} = \delta_{fi} - 2\pi i \delta(E_f - E_i) \\ (\langle q_3\bar{q}_1, q_2\bar{q}_4 | V_{aq_1\bar{q}_2} | q_1\bar{q}_1, q_2\bar{q}_2 \rangle + \langle q_1\bar{q}_4, q_3\bar{q}_2 | V_{a\bar{q}_1q_2} | q_1\bar{q}_1, q_2\bar{q}_2 \rangle), \quad (1)$$

where E_i (E_f) is the total energy of the two initial (final) mesons; $V_{aq_1\bar{q}_2}$ and $V_{a\bar{q}_1q_2}$ are the transition potentials for $q_1 + \bar{q}_2 \rightarrow q_3 + \bar{q}_4$ and $\bar{q}_1 + q_2 \rightarrow q_3 + \bar{q}_4$, respectively; mesons C and D are individually $q_3\bar{q}_1$ and $q_2\bar{q}_4$ in the left diagram and are $q_1\bar{q}_4$ and $q_3\bar{q}_2$ in the right diagram. The wave function of the initial mesons is

$$\psi_{q_1\bar{q}_1, q_2\bar{q}_2} = \frac{e^{i\vec{P}_{q_1\bar{q}_1} \cdot \vec{R}_{q_1\bar{q}_1}}}{\sqrt{V}} \psi_{q_1\bar{q}_1}(\vec{r}_{q_1\bar{q}_1}) \frac{e^{i\vec{P}_{q_2\bar{q}_2} \cdot \vec{R}_{q_2\bar{q}_2}}}{\sqrt{V}} \psi_{q_2\bar{q}_2}(\vec{r}_{q_2\bar{q}_2}), \quad (2)$$

where $\vec{P}_{q_1\bar{q}_1}$ ($\vec{P}_{q_2\bar{q}_2}$), $\vec{R}_{q_1\bar{q}_1}$ ($\vec{R}_{q_2\bar{q}_2}$), and $\vec{r}_{q_1\bar{q}_1}$ ($\vec{r}_{q_2\bar{q}_2}$) are the total momentum, the center-of-mass coordinate, and the relative coordinate of q_1 (q_2) and \bar{q}_1 (\bar{q}_2), respectively. $\psi_{ab}(\vec{r}_{ab})$ is the product of the color wave function, the spin wave function, the flavor wave function, and the relative-motion wave function of constituents a and b . The wave function of the final mesons is

$$\psi_{q_3\bar{q}_1, q_2\bar{q}_4} = \frac{e^{i\vec{P}_{q_3\bar{q}_1} \cdot \vec{R}_{q_3\bar{q}_1}}}{\sqrt{V}} \psi_{q_3\bar{q}_1}(\vec{r}_{q_3\bar{q}_1}) \frac{e^{i\vec{P}_{q_2\bar{q}_4} \cdot \vec{R}_{q_2\bar{q}_4}}}{\sqrt{V}} \psi_{q_2\bar{q}_4}(\vec{r}_{q_2\bar{q}_4}), \quad (3)$$

corresponding to the left diagram, or

$$\psi_{q_1\bar{q}_4, q_3\bar{q}_2} = \frac{e^{i\vec{P}_{q_1\bar{q}_4} \cdot \vec{R}_{q_1\bar{q}_4}}}{\sqrt{V}} \psi_{q_1\bar{q}_4}(\vec{r}_{q_1\bar{q}_4}) \frac{e^{i\vec{P}_{q_3\bar{q}_2} \cdot \vec{R}_{q_3\bar{q}_2}}}{\sqrt{V}} \psi_{q_3\bar{q}_2}(\vec{r}_{q_3\bar{q}_2}), \quad (4)$$

corresponding to the right diagram. $\vec{P}_{q_3\bar{q}_1}$ ($\vec{P}_{q_2\bar{q}_4}$, $\vec{P}_{q_1\bar{q}_4}$, $\vec{P}_{q_3\bar{q}_2}$), $\vec{R}_{q_3\bar{q}_1}$ ($\vec{R}_{q_2\bar{q}_4}$, $\vec{R}_{q_1\bar{q}_4}$, $\vec{R}_{q_3\bar{q}_2}$), and $\vec{r}_{q_3\bar{q}_1}$ ($\vec{r}_{q_2\bar{q}_4}$, $\vec{r}_{q_1\bar{q}_4}$, $\vec{r}_{q_3\bar{q}_2}$) are the total momentum, the center-of-mass coordinate, and the relative coordinate of q_3 and \bar{q}_1 (q_2 and \bar{q}_4 , q_1 and \bar{q}_4 , q_3 and \bar{q}_2), respectively. Every meson wave function is normalized in the volume V .

We first deal with

$$\begin{aligned} & \langle q_3\bar{q}_1, q_2\bar{q}_4 \mid V_{aq_1\bar{q}_2} \mid q_1\bar{q}_1, q_2\bar{q}_2 \rangle \\ &= \int d\vec{r}_{q_1} d\vec{r}_{\bar{q}_1} d\vec{r}_{q_2} d\vec{r}_{q_3} \frac{e^{-i\vec{P}_{q_3\bar{q}_1} \cdot \vec{R}_{q_3\bar{q}_1}}}{\sqrt{V}} \psi_{q_3\bar{q}_1}^+(\vec{r}_{q_3\bar{q}_1}) \frac{e^{-i\vec{P}_{q_2\bar{q}_4} \cdot \vec{R}_{q_2\bar{q}_4}}}{\sqrt{V}} \psi_{q_2\bar{q}_4}^+(\vec{r}_{q_2\bar{q}_4}) \\ & V_{aq_1\bar{q}_2} \frac{e^{i\vec{P}_{q_1\bar{q}_1} \cdot \vec{R}_{q_1\bar{q}_1}}}{\sqrt{V}} \psi_{q_1\bar{q}_1}(\vec{r}_{q_1\bar{q}_1}) \frac{e^{i\vec{P}_{q_2\bar{q}_2} \cdot \vec{R}_{q_2\bar{q}_2}}}{\sqrt{V}} \psi_{q_2\bar{q}_2}(\vec{r}_{q_2\bar{q}_2}). \end{aligned} \quad (5)$$

Let \vec{R}_{total} be the center-of-mass coordinate of the two initial or final mesons, \vec{P}_i (\vec{P}_f) the total three-dimensional momentum of the two initial (final) mesons, and $m_{q_1\bar{q}_1}$ ($m_{q_2\bar{q}_2}$, $m_{q_3\bar{q}_1}$, $m_{q_2\bar{q}_4}$, $m_{q_1\bar{q}_4}$, $m_{q_3\bar{q}_2}$) the mass of $q_1\bar{q}_1$ ($q_2\bar{q}_2$, $q_3\bar{q}_1$, $q_2\bar{q}_4$, $q_1\bar{q}_4$, $q_3\bar{q}_2$). Denote the relative coordinate and the relative momentum of $q_1\bar{q}_1$ and $q_2\bar{q}_2$ by $\vec{r}_{q_1\bar{q}_1, q_2\bar{q}_2}$ and $\vec{p}_{q_1\bar{q}_1, q_2\bar{q}_2}$, respectively. We have

$$\vec{R}_{q_1\bar{q}_1} = \vec{R}_{\text{total}} + \frac{m_{q_2\bar{q}_2}}{m_{q_1\bar{q}_1} + m_{q_2\bar{q}_2}} \vec{r}_{q_1\bar{q}_1, q_2\bar{q}_2}, \quad (6)$$

$$\vec{R}_{q_2\bar{q}_2} = \vec{R}_{\text{total}} - \frac{m_{q_1\bar{q}_1}}{m_{q_1\bar{q}_1} + m_{q_2\bar{q}_2}} \vec{r}_{q_1\bar{q}_1, q_2\bar{q}_2}, \quad (7)$$

$$\vec{P}_{q_1\bar{q}_1} = \frac{m_{q_1\bar{q}_1}}{m_{q_1\bar{q}_1} + m_{q_2\bar{q}_2}} \vec{P}_i + \vec{p}_{q_1\bar{q}_1, q_2\bar{q}_2}, \quad (8)$$

$$\vec{P}_{q_2\bar{q}_2} = \frac{m_{q_2\bar{q}_2}}{m_{q_1\bar{q}_1} + m_{q_2\bar{q}_2}} \vec{P}_i - \vec{p}_{q_1\bar{q}_1, q_2\bar{q}_2}. \quad (9)$$

Denote the relative coordinate and the relative momentum of $q_3\bar{q}_1$ and $q_2\bar{q}_4$ by $\vec{r}_{q_3\bar{q}_1, q_2\bar{q}_4}$ and $\vec{p}_{q_3\bar{q}_1, q_2\bar{q}_4}$, respectively. We have

$$\vec{R}_{q_3\bar{q}_1} = \vec{R}_{\text{total}} + \frac{m_{q_2\bar{q}_4}}{m_{q_3\bar{q}_1} + m_{q_2\bar{q}_4}} \vec{r}_{q_3\bar{q}_1, q_2\bar{q}_4}, \quad (10)$$

$$\vec{R}_{q_2\bar{q}_4} = \vec{R}_{\text{total}} - \frac{m_{q_3\bar{q}_1}}{m_{q_3\bar{q}_1} + m_{q_2\bar{q}_4}} \vec{r}_{q_3\bar{q}_1, q_2\bar{q}_4}, \quad (11)$$

$$\vec{P}_{q_3\bar{q}_1} = \frac{m_{q_3\bar{q}_1}}{m_{q_3\bar{q}_1} + m_{q_2\bar{q}_4}} \vec{P}_f + \vec{p}_{q_3\bar{q}_1, q_2\bar{q}_4}, \quad (12)$$

$$\vec{P}_{q_2\bar{q}_4} = \frac{m_{q_2\bar{q}_4}}{m_{q_3\bar{q}_1} + m_{q_2\bar{q}_4}} \vec{P}_f - \vec{p}_{q_3\bar{q}_1, q_2\bar{q}_4}. \quad (13)$$

From Eqs. (6), (7), (10), and (11) we obtain

$$\vec{r}_{q_1} = \vec{r}_{q_1\bar{q}_1} + \frac{m_{q_2}m_{q_3}}{m_{\bar{q}_1}(m_{q_2} + m_{\bar{q}_4})} \vec{r}_{q_2\bar{q}_4} + \frac{m_{q_3} + m_{\bar{q}_1}}{m_{\bar{q}_1}} \vec{R}_{q_3\bar{q}_1} - \frac{m_{q_3}}{m_{\bar{q}_1}} \vec{R}_{q_2\bar{q}_4}, \quad (14)$$

$$\vec{r}_{\bar{q}_1} = \frac{m_{q_2}m_{q_3}}{m_{\bar{q}_1}(m_{q_2} + m_{\bar{q}_4})} \vec{r}_{q_2\bar{q}_4} + \frac{m_{q_3} + m_{\bar{q}_1}}{m_{\bar{q}_1}} \vec{R}_{q_3\bar{q}_1} - \frac{m_{q_3}}{m_{\bar{q}_1}} \vec{R}_{q_2\bar{q}_4}, \quad (15)$$

$$\vec{r}_{q_2} = \frac{m_{\bar{q}_4}}{m_{q_2} + m_{\bar{q}_4}} \vec{r}_{q_2\bar{q}_4} + \vec{R}_{q_2\bar{q}_4}, \quad (16)$$

$$\vec{r}_{q_3} = -\frac{m_{q_2}}{m_{q_2} + m_{\bar{q}_4}} \vec{r}_{q_2\bar{q}_4} + \vec{R}_{q_2\bar{q}_4}, \quad (17)$$

which lead to

$$\begin{aligned} d\vec{r}_{q_1} d\vec{r}_{\bar{q}_1} d\vec{r}_{q_2} d\vec{r}_{q_3} &= \frac{(m_{q_3} + m_{\bar{q}_1})^3}{m_{\bar{q}_1}^3} d\vec{r}_{q_1\bar{q}_1} d\vec{r}_{q_2\bar{q}_4} d\vec{R}_{q_3\bar{q}_1} d\vec{R}_{q_2\bar{q}_4} \\ &= \frac{(m_{q_3} + m_{\bar{q}_1})^3}{m_{\bar{q}_1}^3} d\vec{r}_{q_1\bar{q}_1} d\vec{r}_{q_2\bar{q}_4} d\vec{r}_{q_3\bar{q}_1, q_2\bar{q}_4} d\vec{R}_{\text{total}}, \end{aligned} \quad (18)$$

where constituent a has the mass m_a and the position vector \vec{r}_a . Eq. (5) becomes

$$\begin{aligned} < q_3\bar{q}_1, q_2\bar{q}_4 \mid V_{aq_1\bar{q}_2} \mid q_1\bar{q}_1, q_2\bar{q}_2 > \\ &= \frac{(m_{q_3} + m_{\bar{q}_1})^3}{m_{\bar{q}_1}^3} \int d\vec{r}_{q_1\bar{q}_1} d\vec{r}_{q_2\bar{q}_4} d\vec{r}_{q_3\bar{q}_1, q_2\bar{q}_4} d\vec{R}_{\text{total}} \\ &\quad \frac{\psi_{q_3\bar{q}_1}^+(\vec{r}_{q_3\bar{q}_1}) \psi_{q_2\bar{q}_4}^+(\vec{r}_{q_2\bar{q}_4})}{\sqrt{V}} e^{-i\vec{P}_f \cdot \vec{R}_{\text{total}} - i\vec{p}_{q_3\bar{q}_1, q_2\bar{q}_4} \cdot \vec{r}_{q_3\bar{q}_1, q_2\bar{q}_4}} \\ &\quad V_{aq_1\bar{q}_2} \frac{\psi_{q_1\bar{q}_1}(\vec{r}_{q_1\bar{q}_1}) \psi_{q_2\bar{q}_2}(\vec{r}_{q_2\bar{q}_2})}{\sqrt{V}} e^{i\vec{P}_i \cdot \vec{R}_{\text{total}} + i\vec{p}_{q_1\bar{q}_1, q_2\bar{q}_2} \cdot \vec{r}_{q_1\bar{q}_1, q_2\bar{q}_2}} \\ &= \frac{(m_{q_3} + m_{\bar{q}_1})^3}{m_{\bar{q}_1}^3} (2\pi)^3 \delta(\vec{P}_f - \vec{P}_i) \int d\vec{r}_{q_1\bar{q}_1} d\vec{r}_{q_2\bar{q}_4} d\vec{r}_{q_3\bar{q}_1, q_2\bar{q}_4} \\ &\quad \frac{\psi_{q_3\bar{q}_1}^+(\vec{r}_{q_3\bar{q}_1}) \psi_{q_2\bar{q}_4}^+(\vec{r}_{q_2\bar{q}_4})}{\sqrt{V}} V_{aq_1\bar{q}_2} \frac{\psi_{q_1\bar{q}_1}(\vec{r}_{q_1\bar{q}_1}) \psi_{q_2\bar{q}_2}(\vec{r}_{q_2\bar{q}_2})}{\sqrt{V}} \\ &\quad e^{i\vec{p}_{q_1\bar{q}_1, q_2\bar{q}_2} \cdot \vec{r}_{q_1\bar{q}_1, q_2\bar{q}_2} - i\vec{p}_{q_3\bar{q}_1, q_2\bar{q}_4} \cdot \vec{r}_{q_3\bar{q}_1, q_2\bar{q}_4}} \\ &= (2\pi)^3 \delta(\vec{P}_f - \vec{P}_i) \frac{\mathcal{M}_{aq_1\bar{q}_2}}{V^2 \sqrt{2E_A 2E_B 2E_C 2E_D}}, \end{aligned} \quad (19)$$

where E_A (E_B , E_C , E_D) is the energy of meson A (B , C , D), and

$$\mathcal{M}_{aq_1\bar{q}_2} = \frac{(m_{q_3} + m_{\bar{q}_1})^3}{m_{\bar{q}_1}^3} \sqrt{2E_A 2E_B 2E_C 2E_D} \int d\vec{r}_{q_1\bar{q}_1} d\vec{r}_{q_2\bar{q}_4} d\vec{r}_{q_3\bar{q}_1, q_2\bar{q}_4}$$

$$\begin{aligned} & \psi_{q_3\bar{q}_1}^+(\vec{r}_{q_3\bar{q}_1})\psi_{q_2\bar{q}_4}^+(\vec{r}_{q_2\bar{q}_4})V_{aq_1\bar{q}_2}\psi_{q_1\bar{q}_1}(\vec{r}_{q_1\bar{q}_1})\psi_{q_2\bar{q}_2}(\vec{r}_{q_2\bar{q}_2}) \\ & e^{i\vec{p}_{q_1\bar{q}_1,q_2\bar{q}_2}\cdot\vec{r}_{q_1\bar{q}_1,q_2\bar{q}_2}-i\vec{p}_{q_3\bar{q}_1,q_2\bar{q}_4}\cdot\vec{r}_{q_3\bar{q}_1,q_2\bar{q}_4}}. \end{aligned} \quad (20)$$

We now address

$$\begin{aligned} & \langle q_1\bar{q}_4, q_3\bar{q}_2 \mid V_{aq_1\bar{q}_2} \mid q_1\bar{q}_1, q_2\bar{q}_2 \rangle \\ &= \int d\vec{r}_{q_1} d\vec{r}_{q_2} d\vec{r}_{\bar{q}_2} d\vec{r}_{q_3} \frac{e^{-i\vec{P}_{q_1\bar{q}_4}\cdot\vec{R}_{q_1\bar{q}_4}}}{\sqrt{V}} \psi_{q_1\bar{q}_4}^+(\vec{r}_{q_1\bar{q}_4}) \frac{e^{-i\vec{P}_{q_3\bar{q}_2}\cdot\vec{R}_{q_3\bar{q}_2}}}{\sqrt{V}} \psi_{q_3\bar{q}_2}^+(\vec{r}_{q_3\bar{q}_2}) \\ & V_{aq_1\bar{q}_2} \frac{e^{i\vec{P}_{q_1\bar{q}_1}\cdot\vec{R}_{q_1\bar{q}_1}}}{\sqrt{V}} \psi_{q_1\bar{q}_1}(\vec{r}_{q_1\bar{q}_1}) \frac{e^{i\vec{P}_{q_2\bar{q}_2}\cdot\vec{R}_{q_2\bar{q}_2}}}{\sqrt{V}} \psi_{q_2\bar{q}_2}(\vec{r}_{q_2\bar{q}_2}). \end{aligned} \quad (21)$$

Let us denote the relative coordinate and the relative momentum of $q_1\bar{q}_4$ and $q_3\bar{q}_2$ by $\vec{r}_{q_1\bar{q}_4,q_3\bar{q}_2}$ and $\vec{p}_{q_1\bar{q}_4,q_3\bar{q}_2}$, respectively. We have

$$\vec{R}_{q_1\bar{q}_4} = \vec{R}_{\text{total}} + \frac{m_{q_3\bar{q}_2}}{m_{q_1\bar{q}_4} + m_{q_3\bar{q}_2}} \vec{r}_{q_1\bar{q}_4,q_3\bar{q}_2}, \quad (22)$$

$$\vec{R}_{q_3\bar{q}_2} = \vec{R}_{\text{total}} - \frac{m_{q_1\bar{q}_4}}{m_{q_1\bar{q}_4} + m_{q_3\bar{q}_2}} \vec{r}_{q_1\bar{q}_4,q_3\bar{q}_2}, \quad (23)$$

$$\vec{P}_{q_1\bar{q}_4} = \frac{m_{q_1\bar{q}_4}}{m_{q_1\bar{q}_4} + m_{q_3\bar{q}_2}} \vec{P}_f + \vec{p}_{q_1\bar{q}_4,q_3\bar{q}_2}, \quad (24)$$

$$\vec{P}_{q_3\bar{q}_2} = \frac{m_{q_3\bar{q}_2}}{m_{q_1\bar{q}_4} + m_{q_3\bar{q}_2}} \vec{P}_f - \vec{p}_{q_1\bar{q}_4,q_3\bar{q}_2}. \quad (25)$$

From Eqs. (6), (7), (22), and (23) we obtain

$$\vec{r}_{q_1} = -\frac{m_{\bar{q}_2}m_{\bar{q}_4}}{m_{q_1}(m_{q_3} + m_{\bar{q}_2})} \vec{r}_{q_3\bar{q}_2} + \frac{m_{q_1} + m_{\bar{q}_4}}{m_{q_1}} \vec{R}_{q_1\bar{q}_4} - \frac{m_{\bar{q}_4}}{m_{\bar{q}_1}} \vec{R}_{q_3\bar{q}_2}, \quad (26)$$

$$\vec{r}_{q_2} = -\vec{r}_{q_1\bar{q}_1} - \frac{m_{\bar{q}_2}m_{\bar{q}_4}}{m_{q_1}(m_{q_3} + m_{\bar{q}_2})} \vec{r}_{q_3\bar{q}_2} + \frac{m_{q_1} + m_{\bar{q}_4}}{m_{q_1}} \vec{R}_{q_1\bar{q}_4} - \frac{m_{\bar{q}_4}}{m_{q_1}} \vec{R}_{q_3\bar{q}_2}, \quad (27)$$

$$\vec{r}_{\bar{q}_2} = -\frac{m_{q_3}}{m_{q_3} + m_{\bar{q}_2}} \vec{r}_{q_3\bar{q}_2} + \vec{R}_{q_3\bar{q}_2}, \quad (28)$$

$$\vec{r}_{q_3} = \frac{m_{\bar{q}_2}}{m_{q_3} + m_{\bar{q}_2}} \vec{r}_{q_3\bar{q}_2} + \vec{R}_{q_3\bar{q}_2}, \quad (29)$$

which lead to

$$\begin{aligned} d\vec{r}_{q_1} d\vec{r}_{q_2} d\vec{r}_{\bar{q}_2} d\vec{r}_{q_3} &= \frac{(m_{q_1} + m_{\bar{q}_4})^3}{m_{q_1}^3} d\vec{r}_{q_1\bar{q}_1} d\vec{r}_{q_3\bar{q}_2} d\vec{R}_{q_1\bar{q}_4} d\vec{R}_{q_3\bar{q}_2} \\ &= \frac{(m_{q_1} + m_{\bar{q}_4})^3}{m_{q_1}^3} d\vec{r}_{q_1\bar{q}_1} d\vec{r}_{q_3\bar{q}_2} d\vec{r}_{q_1\bar{q}_4,q_3\bar{q}_2} d\vec{R}_{\text{total}}. \end{aligned} \quad (30)$$

Then Eq. (21) becomes

$$\begin{aligned}
\langle q_1 \bar{q}_4, q_3 \bar{q}_2 | & V_{a\bar{q}_1 q_2} | q_1 \bar{q}_1, q_2 \bar{q}_2 \rangle \\
&= \frac{(m_{q_1} + m_{\bar{q}_4})^3}{m_{q_1}^3} \int d\vec{r}_{q_1 \bar{q}_1} d\vec{r}_{q_3 \bar{q}_2} d\vec{r}_{q_1 \bar{q}_4, q_3 \bar{q}_2} d\vec{R}_{\text{total}} \\
&\quad \frac{\psi_{q_1 \bar{q}_4}^+(\vec{r}_{q_1 \bar{q}_4})}{\sqrt{V}} \frac{\psi_{q_3 \bar{q}_2}^+(\vec{r}_{q_3 \bar{q}_2})}{\sqrt{V}} e^{-i\vec{P}_f \cdot \vec{R}_{\text{total}} - i\vec{p}_{q_1 \bar{q}_4, q_3 \bar{q}_2} \cdot \vec{r}_{q_1 \bar{q}_4, q_3 \bar{q}_2}} \\
&\quad V_{a\bar{q}_1 q_2} \frac{\psi_{q_1 \bar{q}_1}(\vec{r}_{q_1 \bar{q}_1})}{\sqrt{V}} \frac{\psi_{q_2 \bar{q}_2}(\vec{r}_{q_2 \bar{q}_2})}{\sqrt{V}} e^{i\vec{P}_i \cdot \vec{R}_{\text{total}} + i\vec{p}_{q_1 \bar{q}_1, q_2 \bar{q}_2} \cdot \vec{r}_{q_1 \bar{q}_1, q_2 \bar{q}_2}} \\
&= \frac{(m_{q_1} + m_{\bar{q}_4})^3}{m_{q_1}^3} (2\pi)^3 \delta(\vec{P}_f - \vec{P}_i) \int d\vec{r}_{q_1 \bar{q}_1} d\vec{r}_{q_3 \bar{q}_2} d\vec{r}_{q_1 \bar{q}_4, q_3 \bar{q}_2} \\
&\quad \frac{\psi_{q_1 \bar{q}_4}^+(\vec{r}_{q_1 \bar{q}_4})}{\sqrt{V}} \frac{\psi_{q_3 \bar{q}_2}^+(\vec{r}_{q_3 \bar{q}_2})}{\sqrt{V}} V_{a\bar{q}_1 q_2} \frac{\psi_{q_1 \bar{q}_1}(\vec{r}_{q_1 \bar{q}_1})}{\sqrt{V}} \frac{\psi_{q_2 \bar{q}_2}(\vec{r}_{q_2 \bar{q}_2})}{\sqrt{V}} \\
&\quad e^{i\vec{p}_{q_1 \bar{q}_1, q_2 \bar{q}_2} \cdot \vec{r}_{q_1 \bar{q}_1, q_2 \bar{q}_2} - i\vec{p}_{q_1 \bar{q}_4, q_3 \bar{q}_2} \cdot \vec{r}_{q_1 \bar{q}_4, q_3 \bar{q}_2}} \\
&= (2\pi)^3 \delta(\vec{P}_f - \vec{P}_i) \frac{\mathcal{M}_{a\bar{q}_1 q_2}}{V^2 \sqrt{2E_A 2E_B 2E_C 2E_D}}, \tag{31}
\end{aligned}$$

where

$$\begin{aligned}
\mathcal{M}_{a\bar{q}_1 q_2} &= \frac{(m_{q_1} + m_{\bar{q}_4})^3}{m_{q_1}^3} \sqrt{2E_A 2E_B 2E_C 2E_D} \int d\vec{r}_{q_1 \bar{q}_1} d\vec{r}_{q_3 \bar{q}_2} d\vec{r}_{q_1 \bar{q}_4, q_3 \bar{q}_2} \\
&\quad \psi_{q_1 \bar{q}_4}^+(\vec{r}_{q_1 \bar{q}_4}) \psi_{q_3 \bar{q}_2}^+(\vec{r}_{q_3 \bar{q}_2}) V_{a\bar{q}_1 q_2} \psi_{q_1 \bar{q}_1}(\vec{r}_{q_1 \bar{q}_1}) \psi_{q_2 \bar{q}_2}(\vec{r}_{q_2 \bar{q}_2}) \\
&\quad e^{i\vec{p}_{q_1 \bar{q}_1, q_2 \bar{q}_2} \cdot \vec{r}_{q_1 \bar{q}_1, q_2 \bar{q}_2} - i\vec{p}_{q_1 \bar{q}_4, q_3 \bar{q}_2} \cdot \vec{r}_{q_1 \bar{q}_4, q_3 \bar{q}_2}}. \tag{32}
\end{aligned}$$

Meson i ($i = A, B, C, D$) has the mass m_i , the four-momentum $P_i = (E_i, \vec{P}_i)$, and the angular momentum J_i with its magnetic projection quantum number J_{iz} . The unpolarized cross section for $A + B \rightarrow C + D$ is

$$\begin{aligned}
\sigma^{\text{unpol}}(\sqrt{s}, T) &= \frac{(2\pi)^4}{4\sqrt{(P_A \cdot P_B)^2 - m_A^2 m_B^2}} \int \frac{d^3 P_C}{(2\pi)^3 2E_C} \frac{d^3 P_D}{(2\pi)^3 2E_D} \frac{1}{(2J_A + 1)(2J_B + 1)} \\
&\quad \sum_{J_{Az} J_{Bz} J_{Cz} J_{Dz}} |\mathcal{M}_{a\bar{q}_1 \bar{q}_2} + \mathcal{M}_{a\bar{q}_1 q_2}|^2 \delta(E_f - E_i) \delta(\vec{P}_f - \vec{P}_i), \tag{33}
\end{aligned}$$

where s is the Mandelstam variable given by $s = (E_A + E_B)^2 - (\vec{P}_A + \vec{P}_B)^2$, and T is the temperature. In the center-of-mass frame of A and B the three-dimensional momenta of mesons A and C are \vec{P} and \vec{P}' , respectively. Denote the angle between \vec{P} and \vec{P}' by θ . The unpolarized cross section is given by

$$\sigma^{\text{unpol}}(\sqrt{s}, T) = \frac{1}{(2J_A + 1)(2J_B + 1)} \frac{1}{32\pi s} \frac{|\vec{P}'(\sqrt{s})|}{|\vec{P}(\sqrt{s})|}$$

$$\int_0^\pi d\theta \sum_{J_{Az} J_{Bz} J_{Cz} J_{Dz}} |\mathcal{M}_{aq_1\bar{q}_2} + \mathcal{M}_{a\bar{q}_1q_2}|^2 \sin\theta. \quad (34)$$

III. TRANSITION POTENTIAL

In the reaction $A + B \rightarrow C + D$ the quark of an initial meson annihilates with the antiquark of another meson to produce a gluon, and subsequently this gluon creates a quark to form a final meson and an antiquark to form another final meson. The quark-antiquark annihilation and creation, $q(p_1) + \bar{q}(-p_2) \rightarrow q'(p_3) + \bar{q}'(-p_4)$, is shown in Fig. 2. The initial quark wave function is

$$\psi_q(\vec{p}_1, s_{qz}) = \begin{pmatrix} G_1(\vec{p}_1) \\ \frac{\vec{\sigma} \cdot \vec{p}_1}{2m_q} G_1(\vec{p}_1) \end{pmatrix} \chi_{s_{qz}}, \quad (35)$$

and the final quark wave function is

$$\psi_{q'}(\vec{p}_3, s_{q'z}) = \begin{pmatrix} G_3(\vec{p}_3) \\ \frac{\vec{\sigma} \cdot \vec{p}_3}{2m_{q'}} G_3(\vec{p}_3) \end{pmatrix} \chi_{s_{q'z}}, \quad (36)$$

where $\vec{\sigma}$ are the Pauli matrices; $\chi_{s_{qz}}$ and $\chi_{s_{q'z}}$ are the spin wave functions with the magnetic projection quantum numbers, s_{qz} and $s_{q'z}$, of the quark spin, respectively. The initial antiquark wave function is

$$\psi_{\bar{q}}(\vec{p}_2, s_{\bar{q}z}) = \begin{pmatrix} \frac{\vec{\sigma} \cdot \vec{p}_2}{2m_{\bar{q}}} G_2(\vec{p}_2) \\ G_2(\vec{p}_2) \end{pmatrix} \chi_{s_{\bar{q}z}}, \quad (37)$$

and the final antiquark wave function is

$$\psi_{\bar{q}'}(\vec{p}_4, s_{\bar{q}'z}) = \begin{pmatrix} \frac{\vec{\sigma} \cdot \vec{p}_4}{2m_{\bar{q}'}} G_4(\vec{p}_4) \\ G_4(\vec{p}_4) \end{pmatrix} \chi_{s_{\bar{q}'z}}, \quad (38)$$

where $m_{\bar{q}} = m_q$, $m_{\bar{q}'} = m_{q'}$, and $\chi_{s_{\bar{q}z}}$ and $\chi_{s_{\bar{q}'z}}$ are the spin wave functions with the magnetic projection quantum numbers, $s_{\bar{q}z}$ and $s_{\bar{q}'z}$, of the antiquark spin, respectively. In Eqs. (35)-(38) the color and flavor wave functions are suppressed. According to the Feynman rules given in Ref. [13], the amplitude for the Feynman diagram in Fig. 2 is written as

$$\mathcal{M}_a = \frac{g_s^2}{q^2} \bar{\psi}_{q'}(\vec{p}_3, s_{q'z}) \gamma_\tau T_e \psi_{\bar{q}'}(\vec{p}_4, s_{\bar{q}'z}) \bar{\psi}_{\bar{q}}(\vec{p}_2, s_{\bar{q}z}) \gamma_\tau T_e \psi_q(\vec{p}_1, s_{qz}), \quad (39)$$

where g_s is the gauge coupling constant, T_e ($e = 1, \dots, 8$) are the $SU(3)$ color generators, and $T_e T_e = \frac{\vec{\lambda}(34)}{2} \cdot \frac{\vec{\lambda}(21)}{2}$ with $\vec{\lambda}$ the Gell-Mann matrices. Repeated color and space-time indices (τ) are summed. Using these quark and antiquark wave functions, the amplitude to order of the inverse of the (constituent) quark mass squared is

$$\begin{aligned} \mathcal{M}_a = & \frac{g_s^2}{k^2} \left[\chi_{s_{q'z}}^+ \chi_{s_{\bar{q}z}}^+ T_e T_e G_3(\vec{p}_3) G_2(\vec{p}_2) \frac{\vec{\sigma}(34) \cdot \vec{k} \vec{\sigma}(21) \cdot \vec{k}}{4m_{q'} m_q} G_4(\vec{p}_4) G_1(\vec{p}_1) \chi_{s_{\bar{q}'z}} \chi_{s_{qz}} \right. \\ & - \chi_{s_{q'z}}^+ \chi_{s_{\bar{q}z}}^+ T_e T_e G_3(\vec{p}_3) G_2(\vec{p}_2) \left(\vec{\sigma}(34) \cdot \vec{\sigma}(21) + \frac{\vec{\sigma}(21) \cdot \vec{p}_2 \vec{\sigma}(34) \cdot \vec{\sigma}(21) \vec{\sigma}(21) \cdot \vec{p}_1}{4m_q^2} \right. \\ & \left. \left. + \frac{\vec{\sigma}(34) \cdot \vec{p}_3 \vec{\sigma}(34) \cdot \vec{\sigma}(21) \vec{\sigma}(34) \cdot \vec{p}_4}{4m_{q'}^2} \right) G_4(\vec{p}_4) G_1(\vec{p}_1) \chi_{s_{\bar{q}'z}} \chi_{s_{qz}} \right]. \end{aligned} \quad (40)$$

From the expression of the amplitude we obtain the transition potential for $q(p_1) + \bar{q}(-p_2) \rightarrow q'(p_3) + \bar{q}'(-p_4)$,

$$\begin{aligned} V_{aq\bar{q}}(\vec{k}) = & \frac{g_s^2}{k^2} \frac{\vec{\lambda}(34)}{2} \cdot \frac{\vec{\lambda}(21)}{2} \left(\frac{\vec{\sigma}(34) \cdot \vec{k} \vec{\sigma}(21) \cdot \vec{k}}{4m_{q'} m_q} - \vec{\sigma}(34) \cdot \vec{\sigma}(21) \right. \\ & \left. - \frac{\vec{\sigma}(21) \cdot \vec{p}_2 \vec{\sigma}(34) \cdot \vec{\sigma}(21) \vec{\sigma}(21) \cdot \vec{p}_1}{4m_q^2} - \frac{\vec{\sigma}(34) \cdot \vec{p}_3 \vec{\sigma}(34) \cdot \vec{\sigma}(21) \vec{\sigma}(34) \cdot \vec{p}_4}{4m_{q'}^2} \right), \end{aligned} \quad (41)$$

where $\vec{\lambda}(34)$ ($\vec{\lambda}(21)$) mean that they have matrix elements between the color wave functions of the final (initial) quark and the final (initial) antiquark, and $\vec{\sigma}(34)$ ($\vec{\sigma}(21)$) mean that they have matrix elements between the spin wave functions of the final (initial) quark and the final (initial) antiquark.

IV. TRANSITION AMPLITUDE

In order to obtain the unpolarized cross section, we calculate the transition amplitudes, $\mathcal{M}_{aq_1 \bar{q}_2}$ and $\mathcal{M}_{a\bar{q}_1 q_2}$. We take the Fourier transform of the meson wave functions, $V_{aq_1 \bar{q}_2}$ in Eq. (20), and $V_{a\bar{q}_1 q_2}$ in Eq. (32):

$$\psi_{q_1 \bar{q}_1}(\vec{r}_{q_1 \bar{q}_1}) = \int \frac{d^3 p_{q_1 \bar{q}_1}}{(2\pi)^3} \psi_{q_1 \bar{q}_1}(\vec{p}_{q_1 \bar{q}_1}) e^{i\vec{p}_{q_1 \bar{q}_1} \cdot \vec{r}_{q_1 \bar{q}_1}}, \quad (42)$$

$$\psi_{q_2 \bar{q}_2}(\vec{r}_{q_2 \bar{q}_2}) = \int \frac{d^3 p_{q_2 \bar{q}_2}}{(2\pi)^3} \psi_{q_2 \bar{q}_2}(\vec{p}_{q_2 \bar{q}_2}) e^{i\vec{p}_{q_2 \bar{q}_2} \cdot \vec{r}_{q_2 \bar{q}_2}}, \quad (43)$$

$$\psi_{q_3 \bar{q}_1}(\vec{r}_{q_3 \bar{q}_1}) = \int \frac{d^3 p_{q_3 \bar{q}_1}}{(2\pi)^3} \psi_{q_3 \bar{q}_1}(\vec{p}_{q_3 \bar{q}_1}) e^{i\vec{p}_{q_3 \bar{q}_1} \cdot \vec{r}_{q_3 \bar{q}_1}}, \quad (44)$$

$$\psi_{q_2\bar{q}_4}(\vec{r}_{q_2\bar{q}_4}) = \int \frac{d^3p_{q_2\bar{q}_4}}{(2\pi)^3} \psi_{q_2\bar{q}_4}(\vec{p}_{q_2\bar{q}_4}) e^{i\vec{p}_{q_2\bar{q}_4} \cdot \vec{r}_{q_2\bar{q}_4}}, \quad (45)$$

$$\psi_{q_1\bar{q}_4}(\vec{r}_{q_1\bar{q}_4}) = \int \frac{d^3p_{q_1\bar{q}_4}}{(2\pi)^3} \psi_{q_1\bar{q}_4}(\vec{p}_{q_1\bar{q}_4}) e^{i\vec{p}_{q_1\bar{q}_4} \cdot \vec{r}_{q_1\bar{q}_4}}, \quad (46)$$

$$\psi_{q_3\bar{q}_2}(\vec{r}_{q_3\bar{q}_2}) = \int \frac{d^3p_{q_3\bar{q}_2}}{(2\pi)^3} \psi_{q_3\bar{q}_2}(\vec{p}_{q_3\bar{q}_2}) e^{i\vec{p}_{q_3\bar{q}_2} \cdot \vec{r}_{q_3\bar{q}_2}}, \quad (47)$$

$$V_{aq_1\bar{q}_2}(\vec{r}_{q_3} - \vec{r}_{q_1}) = \int \frac{d^3k}{(2\pi)^3} V_{aq_1\bar{q}_2}(\vec{k}) e^{i\vec{k} \cdot (\vec{r}_{q_3} - \vec{r}_{q_1})}, \quad (48)$$

$$V_{a\bar{q}_1q_2}(\vec{r}_{q_3} - \vec{r}_{q_2}) = \int \frac{d^3k}{(2\pi)^3} V_{a\bar{q}_1q_2}(\vec{k}) e^{i\vec{k} \cdot (\vec{r}_{q_3} - \vec{r}_{q_2})}, \quad (49)$$

where \vec{p}_{ab} is the relative momentum of constituents a and b . The transition amplitudes are then calculated in momentum space by the following expressions:

$$\begin{aligned} \mathcal{M}_{aq_1\bar{q}_2} &= \sqrt{2E_A 2E_B 2E_C 2E_D} \int \frac{d^3p_{q_1\bar{q}_1}}{(2\pi)^3} \frac{d^3p_{q_2\bar{q}_2}}{(2\pi)^3} \\ &\quad \psi_{q_3\bar{q}_1}^+(\vec{p}_{q_3\bar{q}_1}) \psi_{q_2\bar{q}_4}^+(\vec{p}_{q_2\bar{q}_4}) V_{aq_1\bar{q}_2}(\vec{k}) \psi_{q_1\bar{q}_1}(\vec{p}_{q_1\bar{q}_1}) \psi_{q_2\bar{q}_2}(\vec{p}_{q_2\bar{q}_2}), \end{aligned} \quad (50)$$

$$\begin{aligned} \mathcal{M}_{a\bar{q}_1q_2} &= \sqrt{2E_A 2E_B 2E_C 2E_D} \int \frac{d^3p_{q_1\bar{q}_1}}{(2\pi)^3} \frac{d^3p_{q_2\bar{q}_2}}{(2\pi)^3} \\ &\quad \psi_{q_1\bar{q}_4}^+(\vec{p}_{q_1\bar{q}_4}) \psi_{q_3\bar{q}_2}^+(\vec{p}_{q_3\bar{q}_2}) V_{a\bar{q}_1q_2}(\vec{k}) \psi_{q_1\bar{q}_1}(\vec{p}_{q_1\bar{q}_1}) \psi_{q_2\bar{q}_2}(\vec{p}_{q_2\bar{q}_2}). \end{aligned} \quad (51)$$

For convenience sake we also use the notation ψ_A , ψ_B , ψ_C , and ψ_D : $\psi_A = \psi_{q_1\bar{q}_1}$, $\psi_B = \psi_{q_2\bar{q}_2}$, $\psi_C = \psi_{q_3\bar{q}_1} = \psi_{q_1\bar{q}_4}$, and $\psi_D = \psi_{q_2\bar{q}_4} = \psi_{q_3\bar{q}_2}$. The wave functions of mesons A , B , C , and D are individually given by

$$\psi_A = \phi_{A\text{rel}} \phi_{A\text{color}} \phi_{A\text{flavor}} \chi_{S_A S_{Az}}, \quad (52)$$

$$\psi_B = \phi_{B\text{rel}} \phi_{B\text{color}} \phi_{B\text{flavor}} \chi_{S_B S_{Bz}}, \quad (53)$$

$$\psi_C = \phi_{C\text{rel}} \phi_{C\text{color}} \phi_{C\text{flavor}} \chi_{S_C S_{Cz}}, \quad (54)$$

$$\psi_D = \phi_{D\text{rel}} \phi_{D\text{color}} \phi_{D\text{flavor}} \chi_{S_D S_{Dz}}, \quad (55)$$

where $\phi_{A\text{rel}}$ ($\phi_{B\text{rel}}$, $\phi_{C\text{rel}}$, $\phi_{D\text{rel}}$), $\phi_{A\text{color}}$ ($\phi_{B\text{color}}$, $\phi_{C\text{color}}$, $\phi_{D\text{color}}$), $\phi_{A\text{flavor}}$ ($\phi_{B\text{flavor}}$, $\phi_{C\text{flavor}}$, $\phi_{D\text{flavor}}$), and $\chi_{S_A S_{Az}}$ ($\chi_{S_B S_{Bz}}$, $\chi_{S_C S_{Cz}}$, $\chi_{S_D S_{Dz}}$) are the quark-antiquark relative-motion wave function, the color wave function, the flavor wave function, and the spin wave function of meson A (B , C , D), respectively. The spin of meson A (B , C , D) is S_A

(S_B, S_C, S_D) with its magnetic projection quantum number S_{Az} (S_{Bz}, S_{Cz}, S_{Dz}). The transition amplitudes contain color, spin, and flavor matrix elements. The color matrix element is

$$\mathcal{M}_{aq_1\bar{q}_2c} = \phi_{C\text{color}}^+ \phi_{D\text{color}}^+ \frac{\vec{\lambda}(34)}{2} \cdot \frac{\vec{\lambda}(21)}{2} \phi_{A\text{color}} \phi_{B\text{color}} = \frac{4}{9}, \quad (56)$$

for the left diagram of Fig. 1, and

$$\mathcal{M}_{a\bar{q}_1q_2c} = \phi_{C\text{color}}^+ \phi_{D\text{color}}^+ \frac{\vec{\lambda}(34)}{2} \cdot \frac{\vec{\lambda}(12)}{2} \phi_{A\text{color}} \phi_{B\text{color}} = \frac{4}{9}, \quad (57)$$

for the right diagram of Fig. 1. The transition potential in Eq. (41) includes the Pauli matrices $\vec{\sigma}(21)$ and $\vec{\sigma}(34)$. The spin matrix elements of the Pauli matrices involved in the left diagram are listed in Tables 1-14. The matrix elements of $\sigma_1(21)$, $\sigma_3(21)$, $\sigma_1(34)$, $\sigma_3(34)$, $\sigma_1(21)\sigma_1(34)$, $\sigma_1(21)\sigma_3(34)$, $\sigma_2(21)\sigma_2(34)$, $\sigma_3(21)\sigma_1(34)$, and $\sigma_3(21)\sigma_3(34)$ are real, and the matrix elements of $\sigma_2(21)$, $\sigma_2(34)$, $\sigma_1(21)\sigma_2(34)$, $\sigma_2(21)\sigma_1(34)$, $\sigma_2(21)\sigma_3(34)$, and $\sigma_3(21)\sigma_2(34)$ are pure imaginary or zero. The spin matrix elements for the right diagram in Fig. 1 can be obtained from the ones for the left diagram. The real (imaginary) spin matrix elements of $\mathcal{M}_{a\bar{q}_1q_2}$ equal the real spin matrix elements (equal the negative of the imaginary spin matrix elements) of $\mathcal{M}_{aq_1\bar{q}_2}$, while none, two, or four of the initial and final mesons have zero spins. The real (imaginary) spin matrix elements of $\mathcal{M}_{a\bar{q}_1q_2}$ equal the negative of the real spin matrix elements (equal the imaginary spin matrix elements) of $\mathcal{M}_{aq_1\bar{q}_2}$, when one or three of the initial and final mesons have zero spins.

The flavor states, $\phi_{A\text{flavor}}$ and $\phi_{B\text{flavor}}$, are coupled to the flavor state $|AB, I, I_z\rangle$ with the total isospin I and its magnetic projection quantum number I_z . $\phi_{C\text{flavor}}$ and $\phi_{D\text{flavor}}$ are coupled to $|CD, I, I_z\rangle$. The flavor matrix element is

$$\mathcal{M}_{aq_1\bar{q}_2f} = \langle CD, I, I_z | P_{q_1+\bar{q}_2 \rightarrow q_3+\bar{q}_4} | AB, I, I_z \rangle, \quad (58)$$

for the left diagram of Fig. 1, and

$$\mathcal{M}_{a\bar{q}_1q_2f} = \langle CD, I, I_z | P_{\bar{q}_1+q_2 \rightarrow q_3+\bar{q}_4} | AB, I, I_z \rangle, \quad (59)$$

for the right diagram of Fig. 1. The symbol $P_{q_1+\bar{q}_2 \rightarrow q_3+\bar{q}_4}$ ($P_{\bar{q}_1+q_2 \rightarrow q_3+\bar{q}_4}$) is the operator that implements $q_1 + \bar{q}_2 \rightarrow q_3 + \bar{q}_4$ ($\bar{q}_1 + q_2 \rightarrow q_3 + \bar{q}_4$) in flavor space. $\mathcal{M}_{a\bar{q}_1q_2f}$ may differ

from $\mathcal{M}_{aq_1\bar{q}_2f}$. In Table 15 the flavor matrix elements for the reactions are listed:

$$\pi\pi \rightarrow \rho\rho, \quad K\bar{K} \rightarrow K^*\bar{K}^*, \quad K\bar{K}^* \rightarrow K^*\bar{K}^*, \quad K^*\bar{K} \rightarrow K^*\bar{K}^*,$$

$$\pi\pi \rightarrow K\bar{K}, \quad \pi\rho \rightarrow K\bar{K}^*, \quad \pi\rho \rightarrow K^*\bar{K}, \quad K\bar{K} \rightarrow \rho\rho.$$

We use the following notation, $K = \begin{pmatrix} K^+ \\ K^0 \end{pmatrix}$, $\bar{K} = \begin{pmatrix} \bar{K}^0 \\ K^- \end{pmatrix}$, $K^* = \begin{pmatrix} K^{*+} \\ K^{*0} \end{pmatrix}$, and $\bar{K}^* = \begin{pmatrix} \bar{K}^{*0} \\ K^{*-} \end{pmatrix}$. Let us give an example that shows how to obtain the flavor matrix elements listed in Table 15. The example is $\pi\pi \rightarrow K\bar{K}$ for $I = 1$. The initial and final flavor states are given by

$$|\pi\pi, I = 1, I_z = -1\rangle = \frac{1}{\sqrt{2}}(|\pi^0\rangle|\pi^- \rangle - |\pi^- \rangle|\pi^0 \rangle), \quad (60)$$

$$|\pi\pi, I = 1, I_z = 0\rangle = \frac{1}{\sqrt{2}}(|\pi^+\rangle|\pi^- \rangle - |\pi^- \rangle|\pi^+ \rangle), \quad (61)$$

$$|\pi\pi, I = 1, I_z = 1\rangle = \frac{1}{\sqrt{2}}(|\pi^+\rangle|\pi^0 \rangle - |\pi^0 \rangle|\pi^+ \rangle), \quad (62)$$

$$|K\bar{K}, I = 1, I_z = -1\rangle = |K^0\rangle|K^- \rangle, \quad (63)$$

$$|K\bar{K}, I = 1, I_z = 0\rangle = \frac{1}{\sqrt{2}}(|K^+\rangle|K^- \rangle + |K^0\rangle|\bar{K}^0 \rangle), \quad (64)$$

$$|K\bar{K}, I = 1, I_z = 1\rangle = |K^+\rangle|\bar{K}^0 \rangle. \quad (65)$$

The flavor wave functions of the pion and kaon are $|\pi^+\rangle = -|\bar{u}d\rangle$, $|\pi^0\rangle = \frac{1}{\sqrt{2}}(|u\bar{u}\rangle - |d\bar{d}\rangle)$, $|\pi^-\rangle = |\bar{d}u\rangle$, $|K^+\rangle = |u\bar{s}\rangle$, $|K^0\rangle = |d\bar{s}\rangle$, $|\bar{K}^0\rangle = -|s\bar{d}\rangle$, $|K^-\rangle = |s\bar{u}\rangle$. The flavor matrix elements for $\pi\pi \rightarrow K\bar{K}$ for $I = 1$ are $\mathcal{M}_{aq_1\bar{q}_2f} = 0$ and $\mathcal{M}_{a\bar{q}_1q_2f} = -1$, which are independent of I_z . This indicates that only the right diagram in Fig. 1 contributes to $\pi\pi \rightarrow K\bar{K}$ for $I = 1$.

V. QUARK-ANTIQUARK RELATIVE-MOTION WAVE FUNCTIONS

The mesonic quark-antiquark relative-motion wave functions in coordinate space are solutions of the Schrödinger equation with the potential in the medium [14]:

$$V(\vec{r}) = V_{\text{si}}(\vec{r}) + V_{\text{ss}}(\vec{r}), \quad (66)$$

where \vec{r} is the relative coordinate of the quark and the antiquark inside the meson. V_{si} is the central spin-independent potential,

$$V_{\text{si}}(\vec{r}) = D \left[1.3 - \left(\frac{T}{T_c} \right)^4 \right] \tanh(Ar) - \frac{8\pi}{25} \frac{v(\lambda r)}{r} \exp(-Er), \quad (67)$$

where $D = 0.7$ GeV, $T_c = 0.175$ GeV, $A = 1.5[0.75 + 0.25(T/T_c)^{10}]^6$ GeV, $E = 0.6$ GeV, $\lambda = \sqrt{25/16\pi^2\alpha'}$ with $\alpha' = 1.04$ GeV⁻², and $v(x)$ is

$$v(x) = \frac{100}{3\pi} \int_0^\infty \frac{dQ}{Q} \left[\rho(\vec{Q}^2) - \frac{K}{\vec{Q}^2} \right] \sin\left(\frac{Q}{\lambda}x\right), \quad (68)$$

where $K = 3/16\pi^2\alpha'$ and $\rho(\vec{Q}^2)$ is given by Buchmüller and Tye [15]. At short distances the quark interaction is described by perturbative QCD in vacuum, and one-gluon exchange plus perturbative one- and two-loop corrections gives the quark-antiquark potential $-\frac{8\pi}{25} \frac{v(\lambda r)}{r}$ [15]. Medium screening sets in at distances $r \geq 0.3$ fm. Including medium effects lattice QCD calculations have provided the numerical quark-antiquark potential at intermediate and long distances [16], which depends on the temperature of the medium. The potential $V_{\text{si}}(\vec{r})$ fits rather well $-\frac{8\pi}{25} \frac{v(\lambda r)}{r}$ at short distances and the numerical potential at intermediate and long distances.

Starting with Feynman diagrams for elastic particle-particle scattering, one gets a relativistic particle-particle potential. Application of the Foldy-Wouthuysen canonical transformation to the two-particle relativistic Hamiltonian with the relativistic potential leads to a nonrelativistic particle-particle potential that includes a central spin-independent potential, a spin-spin interaction, and other terms [17]. This standard procedure for obtaining the nonrelativistic particle-particle potential is the same for heavy or light particles. In other words, the particle-particle potential is valid no matter how light the particles are. This procedure has been successfully applied and tested to get the electron-electron potential arising from propagation of a space-like photon [18], the short-distance quark-quark potential arising from propagation of a space-like gluon [19], and so on. Thus, the first term in Eq. (67), obtained in lattice calculations involving a heavy quark and a heavy antiquark, is reasonably applied to a light constituent quark and a light constituent antiquark as well.

The second term in Eq. (66) is the spin-spin interaction that arises from perturbative one-gluon exchange plus one- and two-loop corrections [20] and includes relativistic effects [3, 21]:

$$V_{\text{ss}}(\vec{r}) = \frac{64\pi^2}{75} \frac{d^3}{\pi^{3/2}} \exp(-d^2 r^2) \frac{\vec{s}_a \cdot \vec{s}_b}{m_a m_b} - \frac{16\pi}{75} \frac{1}{r} \frac{d^2 v(\lambda r)}{dr^2} \frac{\vec{s}_a \cdot \vec{s}_b}{m_a m_b}, \quad (69)$$

where \vec{s}_a is the spin of constituent a , and the quantity d is given by

$$d^2 = \sigma_0^2 \left[\frac{1}{2} + \frac{1}{2} \left(\frac{4m_a m_b}{(m_a + m_b)^2} \right)^4 \right] + \sigma_1^2 \left(\frac{2m_a m_b}{m_a + m_b} \right)^2, \quad (70)$$

where $\sigma_0 = 0.15$ GeV and $\sigma_1 = 0.705$.

With up quark mass 0.32 GeV, down quark mass 0.32 GeV, strange quark mass 0.5 GeV, and charm quark mass 1.51 GeV, the Schrödinger equation with the potential given in Eq. (66) at $T = 0$ is solved to reproduce the experimental masses of π , ρ , K , K^* , J/ψ , ψ' , χ_c , D , D^* , D_s , and D_s^* mesons [22]. The elastic $\pi\pi$ scattering for $I = 2$ is governed by the quark-interchange process. The experimental data of S -wave phase shifts for the scattering in vacuum [23–26] are reproduced in the Born approximation together with the pionic quark-antiquark relative-motion wave functions obtained from the Schrödinger equation [14].

VI. NUMERICAL CROSS SECTIONS AND DISCUSSIONS

We are now ready to calculate elastic phase shifts for $\pi\pi$ scattering in vacuum. From the transition amplitudes we get the reduced T -matrix element,

$$T_{\text{fi}} = \frac{\mathcal{M}_{a q_1 \bar{q}_2} + \mathcal{M}_{a \bar{q}_1 q_2}}{(2\pi)^3 \sqrt{2E_A 2E_B 2E_C 2E_D}}. \quad (71)$$

The phase shift for $A + B \rightarrow A + B$ is

$$\exp(i\delta_l) \sin \delta_l = -\frac{2\pi^2}{E_A + E_B} \left| \vec{P} \right| \frac{E_A E_B}{E_A + E_B} \int_{-1}^1 dx T_{\text{fi}} P_l(x), \quad (72)$$

where $x = \cos \theta$, and P_l are the Legendre polynomials. The elastic phase shift is calculated by the expression,

$$\delta_l = -\frac{1}{2} \arcsin \text{Re} \left[\frac{4\pi^2}{E_A + E_B} \left| \vec{P} \right| \frac{E_A E_B}{E_A + E_B} \int_{-1}^1 dx T_{\text{fi}} P_l(x) \right]. \quad (73)$$

The S -wave $I = 0$ and P -wave $I = 1$ elastic phase shifts for $\pi\pi$ scattering in vacuum are shown respectively in Figs. 3 and 4 and compared with the experimental data [27–35].

When the S -wave $I = 0$ elastic phase shift is larger than 30 degree, it increases rapidly with increasing \sqrt{s} . This behavior is already known from results of chiral perturbation theory [36,37] and the result of the master formula approach [38]. The experimental data of P -wave $I = 1$ elastic phase shifts for $\pi\pi$ scattering in vacuum cannot be reproduced. This is because resonances are not included in the present approach. This is similar to the tree calculation in chiral perturbation theory [36]. Including one- and two-loop corrections in chiral perturbation theory and imposing unitarity, the resonances appear and the experimental data are reproduced. This has been shown in approaches based on the results of chiral perturbation theory, for example, the master formula approach [38], the Padé method [39], the large- N_f expansion [40], the N/D method [41], the inverse amplitude method [42], the K -matrix method [43], the current algebra unitarization [44], the Roy equations [45], the coupled-channel Lippmann-Schwinger equations [46], the Bethe-Salpeter approach [47], and the approaches based on effective meson Lagrangians [48–55].

We consider the following inelastic meson-meson scattering processes that are governed by quark-antiquark annihilation and creation:

$$I = 1 \pi\pi \rightarrow \rho\rho, \quad K\bar{K} \rightarrow K^*\bar{K}^*, \quad K\bar{K}^* \rightarrow K^*\bar{K}^*, \quad K^*\bar{K} \rightarrow K^*\bar{K}^*,$$

$$I = 1 \pi\pi \rightarrow K\bar{K}, \quad \pi\rho \rightarrow K\bar{K}^*, \quad \pi\rho \rightarrow K^*\bar{K}, \quad K\bar{K} \rightarrow \rho\rho.$$

The quark-antiquark relative-motion wave functions, $\phi_{A\text{rel}}$, $\phi_{B\text{rel}}$, $\phi_{C\text{rel}}$, and $\phi_{D\text{rel}}$, are obtained from the Schrödinger equation with the potential given in Eq. (66). With the transition potential and the wave functions in Eqs. (52)–(55), we calculate the transition amplitudes, $\mathcal{M}_{a\bar{q}_1\bar{q}_2}$ and $\mathcal{M}_{a\bar{q}_1q_2}$. According to Eq. (34) we calculate unpolarized cross sections at the six temperatures $T/T_c = 0, 0.65, 0.75, 0.85, 0.9$, and 0.95 . In Figs. 5–13 we plot the unpolarized cross sections for the nine channels:

$$I = 1 \pi\pi \rightarrow \rho\rho, \quad I = 1 K\bar{K} \rightarrow K^*\bar{K}^*, \quad I = 0 K\bar{K} \rightarrow K^*\bar{K}^*,$$

$$I = 1 K\bar{K}^* \rightarrow K^*\bar{K}^*, \quad I = 0 K\bar{K}^* \rightarrow K^*\bar{K}^*, \quad I = 1 \pi\pi \rightarrow K\bar{K},$$

$$I = 1 \pi\rho \rightarrow K\bar{K}^*, \quad I = 1 \pi\rho \rightarrow K^*\bar{K}, \quad I = 1 K\bar{K} \rightarrow \rho\rho.$$

Depending on temperature, a reaction is either endothermic or exothermic. The numerical cross sections for endothermic reactions are parametrized as

$$\begin{aligned} \sigma^{\text{unpol}}(\sqrt{s}, T) = & a_1 \left(\frac{\sqrt{s} - \sqrt{s_0}}{b_1} \right)^{c_1} \exp \left[c_1 \left(1 - \frac{\sqrt{s} - \sqrt{s_0}}{b_1} \right) \right] \\ & + a_2 \left(\frac{\sqrt{s} - \sqrt{s_0}}{b_2} \right)^{c_2} \exp \left[c_2 \left(1 - \frac{\sqrt{s} - \sqrt{s_0}}{b_2} \right) \right], \end{aligned} \quad (74)$$

where $\sqrt{s_0}$ is the threshold energy, and a_1 , b_1 , c_1 , a_2 , b_2 , and c_2 are parameters. The numerical cross sections for exothermic reactions are parametrized as

$$\begin{aligned} \sigma^{\text{unpol}}(\sqrt{s}, T) = & \frac{\vec{P}^{\prime 2}}{\vec{P}^2} \left\{ a_1 \left(\frac{\sqrt{s} - \sqrt{s_0}}{b_1} \right)^{c_1} \exp \left[c_1 \left(1 - \frac{\sqrt{s} - \sqrt{s_0}}{b_1} \right) \right] \right. \\ & \left. + a_2 \left(\frac{\sqrt{s} - \sqrt{s_0}}{b_2} \right)^{c_2} \exp \left[c_2 \left(1 - \frac{\sqrt{s} - \sqrt{s_0}}{b_2} \right) \right] \right\}. \end{aligned} \quad (75)$$

The parameter values are listed in Tables 16-18. As in Ref. [2], we also list the quantities d_0 and $\sqrt{s_z}$; d_0 is the separation between the peak's location on the \sqrt{s} -axis and the threshold energy, and $\sqrt{s_z}$ is the square root of the Mandelstam variable at which the cross section is 1/100 of the peak cross section.

In the temperature region that is covered by hadronic matter produced in ultrarelativistic heavy-ion collisions, the central spin-independent potential given in Eq. (67) at long distances becomes independent of distance and exhibits a plateau. Confinement is marked by the plateau. With increasing temperature the height of the plateau decreases, confinement becomes weaker and weaker, and quark-antiquark bound states become looser and looser. Increasing radii of mesons A and B cause increasing cross sections for meson-meson reactions. Weakening confinement causes the combination of final quarks and antiquarks in forming mesons C and D to be more difficult, thus decreasing cross sections for meson-meson reactions. The two factors determine the decrease or the increase of peak cross sections of endothermic reactions shown in Figs. 5-13. For example, from $T/T_c = 0$ to 0.85 and near the threshold energy the increase of the cross section due to increasing radii of initial mesons cannot overcome the decrease of the cross section due to weakening confinement. Thus, the peak cross section of $K\bar{K} \rightarrow K^*\bar{K}^*$ decreases. In contrast, the peak cross section of $K\bar{K} \rightarrow K^*\bar{K}^*$ increases as temperature goes from $T/T_c = 0.85$ to 0.95. In vacuum the ρ mass is larger than the kaon mass. When the

temperature increases, the ρ mass decreases faster than the kaon mass. At $T \simeq 0.785T_c$ the ρ mass equals the kaon mass. Below this temperature the reaction $K\bar{K} \rightarrow \rho\rho$ for $I = 1$ in Fig. 13 is endothermic; otherwise, it is exothermic. When temperature increases from $T/T_c = 0.6$ to 1, the π , ρ , K , and K^* masses decrease. The threshold energies shown in Figs. 5-13 thus decrease. The ratio of the peak cross section at $T/T_c=0.75$ to the peak cross section at $T/T_c=0$ is 0.08, 0.34, 0.25, 0.16, 0.19, 0.11, 0.05, and 0.13 for $\pi\pi \rightarrow \rho\rho$ for $I = 1$, $K\bar{K} \rightarrow K^*\bar{K}^*$ for $I = 1$, $K\bar{K} \rightarrow K^*\bar{K}^*$ for $I = 0$, $K\bar{K}^* \rightarrow K^*\bar{K}^*$ for $I = 1$, $K\bar{K}^* \rightarrow K^*\bar{K}^*$ for $I = 0$, $\pi\rho \rightarrow K\bar{K}^*$ for $I = 1$, $\pi\rho \rightarrow K^*\bar{K}$ for $I = 1$, and $K\bar{K} \rightarrow \rho\rho$ for $I = 1$, respectively. Clearly, the cross sections have remarkable dependence on temperature.

It is shown in Table 15 that the two diagrams in Fig. 1 contribute to $K\bar{K} \rightarrow K^*\bar{K}^*$ for $I = 0$ and $K\bar{K}^* \rightarrow K^*\bar{K}^*$ for $I = 0$, and only the right diagram contributes to $K\bar{K} \rightarrow K^*\bar{K}^*$ for $I = 1$ and $K\bar{K}^* \rightarrow K^*\bar{K}^*$ for $I = 1$. The peak cross section of $K\bar{K} \rightarrow K^*\bar{K}^*$ ($K\bar{K}^* \rightarrow K^*\bar{K}^*$) for $I = 0$ at a given temperature is more than 2 times the one for $I = 1$. In addition, cross sections for $K^*\bar{K} \rightarrow K^*\bar{K}^*$ equal the cross sections for $K\bar{K}^* \rightarrow K^*\bar{K}^*$.

It is shown in Table 15 that only the right diagram in Fig. 1 contributes to the reactions, $\pi\pi \rightarrow K\bar{K}$, $\pi\rho \rightarrow K\bar{K}^*$, $\pi\rho \rightarrow K^*\bar{K}$, and $K\bar{K} \rightarrow \rho\rho$. Since the flavor matrix element for the channel $I = 0$ is $-\sqrt{6}/2$ times the one for $I = 1$, the cross section for the channel $I = 0$ is 1.5 times the one for $I = 1$. Therefore, we only plot the unpolarized cross sections for $\pi\pi \rightarrow K\bar{K}$ for $I = 1$ in Fig. 10, for $\pi\rho \rightarrow K\bar{K}^*$ for $I = 1$ in Fig. 11, for $\pi\rho \rightarrow K^*\bar{K}$ for $I = 1$ in Fig. 12, and for $K\bar{K} \rightarrow \rho\rho$ for $I = 1$ in Fig. 13. The cross section for $\pi\rho \rightarrow K\bar{K}^*$ at $T = 0$ leads to the isospin-averaged cross section that has a maximum value of about 0.36 mb which is close to the one obtained from an effective meson Lagrangian in Refs. [4, 6]. Nevertheless, the cross section for $K\bar{K} \rightarrow \rho\rho$ at $T = 0$ provides about 1 mb as the maximum value of the isospin-averaged cross section, which is not close to 3.5 mb given in Refs. [4, 6].

The unpolarized cross section for $\pi\pi \rightarrow \rho\rho$ for $I = 2$ has been shown in Fig. 2 of Ref. [2]. The channel is governed by the quark-interchange process. The reaction $\pi\pi \rightarrow \rho\rho$ for $I = 1$

studied in the present work is governed by quark-antiquark annihilation and creation. The unpolarized cross sections for both channels increase rapidly when \sqrt{s} increases from the threshold energy. When \sqrt{s} increases from the magnitude that corresponds to the peak cross section, the cross section for the channel $I = 2$ decreases rapidly, but the one for $I = 1$ decreases slowly. The difference is related to the quark-antiquark relative-motion wave functions of final mesons. The wave functions are exponentially decreasing functions of the quark-antiquark relative momentum. When \sqrt{s} is far away from the threshold energy, the relative momentum of an interchanged quark and an antiquark, which form a final meson in the channel $I = 2$, is usually large [1], but the relative momentum of the quark created from the gluon and an antiquark, which form a final meson in the channel $I = 1$, can still be small. The squared transition amplitude for the reaction with the quark-interchange process at such a value of \sqrt{s} is very small in comparison to the one near the threshold energy, and by contrast the squared transition amplitude for the reaction with the quark-antiquark annihilation is comparable to the one near the threshold energy. Therefore, the cross section has the behavior of rapid decrease for $I = 2$ and of slow decrease for $I = 1$, and the difference between the cross sections for the two channels is large.

VII. SUMMARY

We have derived the unpolarized cross section for inelastic meson-meson scattering in quark degrees of freedom. The reactions are governed by quark-antiquark annihilation and creation. The reactions include $\pi\pi \rightarrow \rho\rho$ for $I = 1$, $K\bar{K} \rightarrow K^*\bar{K}^*$, $K\bar{K}^* \rightarrow K^*\bar{K}$, $K^*\bar{K} \rightarrow K^*\bar{K}^*$, $\pi\pi \rightarrow K\bar{K}$ for $I = 1$, $\pi\rho \rightarrow K\bar{K}^*$, $\pi\rho \rightarrow K^*\bar{K}$, and $K\bar{K} \rightarrow \rho\rho$. The transition potential corresponding to quark-antiquark annihilation and creation has been derived in perturbative QCD. Some reactions involve only one Feynman diagram at tree level, and the others two. The transition amplitudes including color, spin, and flavor matrix elements are given upon integrating over the relative momenta of the quark and the antiquark of the two initial mesons. The experimental data of S -wave and P -wave elastic phase shifts for $\pi\pi$ scattering near the threshold energy can be accounted

for by quark-antiquark annihilation and creation in the Born approximation. Numerical unpolarized cross sections have been obtained at the six temperatures and have shown remarkable temperature dependence. The dependence arises from the quark-antiquark relative-motion wave functions of the initial and final mesons. The numerical cross sections are parametrized for future use in the evolution of hadronic matter.

ACKNOWLEDGEMENTS

We thank W. Weise for introducing us to his work and B. S. Zou for helpful discussions on meson-meson reactions. This work was supported by the National Natural Science Foundation of China under Grant No. 11175111.

References

- [1] Y.-Q. Li and X.-M. Xu, Nucl. Phys. A 794, 210 (2007).
- [2] Z.-Y. Shen and X.-M. Xu, J. Korean Phys. Soc. 66, 754 (2015).
- [3] T. Barnes and E. S. Swanson, Phys. Rev. D 46, 131 (1992); E. S. Swanson, Ann. Phys. (N.Y.) 220, 73 (1992).
- [4] G. E. Brown, C. M. Ko, Z. G. Wu, and L. H. Xia, Phys. Rev. C 43, 1881 (1991).
- [5] S. A. Bass *et al.*, Prog. Part. Nucl. Phys. 41, 255 (1998); C. Nonaka and S. A. Bass, Phys. Rev. C 75, 014902 (2007).
- [6] W. Cassing, E. L. Bratkovskaya, U. Mosel, S. Teis, and A. Sibirtsev, Nucl. Phys. A 614, 415 (1997).
- [7] Y.-Q. Li, X.-M. Xu, and H.-J. Ge, Eur. Phys. J. A 47, 65 (2011).
- [8] M. Kohno and W. Weise, Nucl. Phys. A 454, 429 (1986); Nucl. Phys. A 479, 433c (1988).

- [9] R. Tegen, T. Mizutani, and F. Myhrer, Phys. Rev. D 32, 1672 (1985); F. Myhrer and R. Tegen, Phys. Lett. B 162, 237 (1985).
- [10] J. Haidenbauer, T. Hippchen, and R. Tegen, Phys. Rev. C 44, 1812 (1991); J. Haidenbauer, K. Holinde, V. Mull, and J. Speth, Phys. Rev. C 46, 2158 (1992).
- [11] C. B. Dover and P. M. Fishbane, Nucl. Phys. B 244, 349 (1984); Phys. Rev. Lett. 62, 2917 (1989).
- [12] M. Maruyama, S. Furui, and A. Faessler, Nucl. Phys. A 472, 643 (1987); A. Muhm, T. Gutsche, R. Thierauf, Y. Yan, and A. Faessler, Nucl. Phys. A 598, 285 (1996).
- [13] T. Muta, *Foundations of Quantum Chromodynamics* (World Scientific, Singapore, 1987).
- [14] S.-T. Ji, Z.-Y. Shen, and X.-M. Xu, J. Phys. G 42, 095110 (2015).
- [15] W. Buchmüller and S.-H. H. Tye, Phys. Rev. D 24, 132 (1981).
- [16] F. Karsch, E. Laermann, and A. Peikert, Nucl. Phys. B 605, 579 (2001).
- [17] Z. V. Chraplyvy, Phys. Rev. 91, 388 (1953); Phys. Rev. 92, 1310 (1953).
- [18] M. A. Strosio, Phys. Rep. 22 C, 215 (1975).
- [19] A. De Rújula, H. Georgi, and S. L. Glashow, Phys. Rev. D 12, 147 (1975).
- [20] X.-M. Xu, Nucl. Phys. A 697, 825 (2002).
- [21] S. Godfrey and N. Isgur, Phys. Rev. D 32, 189 (1985).
- [22] K. Nakamura *et al.* (Particle Data Group), J. Phys. G 37, 075021 (2010).
- [23] E. Colton *et al.*, Phys. Rev. D 3, 2028 (1971).
- [24] N. B. Durusoy *et al.*, Phys. Lett. B 45, 517 (1973).
- [25] M. J. Losty *et al.*, Nucl. Phys. B 69, 185 (1974).

- [26] W. Hoogland *et al.*, Nucl. Phys. B 126, 109 (1977).
- [27] S. D. Protopopescu *et al.*, Phys. Rev. D 7, 1279 (1973).
- [28] B. Hyams *et al.*, Nucl. Phys. B 64, 134 (1973).
- [29] P. Estabrooks and A. D. Martin, Nucl. Phys. B 79, 301 (1974).
- [30] V. Srinivasan *et al.*, Phys. Rev. D 12, 681 (1975).
- [31] L. Rosselet *et al.*, Phys. Rev. D 15, 574 (1977).
- [32] C. D. Froggatt and J. L. Petersen, Nucl. Phys. B 129, 89 (1977).
- [33] A. A. Bel'kol *et al.*, JETP Lett. 29, 597 (1979).
- [34] E. A. Alekseeva *et al.*, Sov. Phys. JETP 55, 591 (1982).
- [35] R. García-Martín, R. Kamiński, J. R. Peláez, J. R. de Elvira, and F. J. Ynduráin, Phys. Rev. D 83, 074004 (2011).
- [36] J. Gasser and H. Leutwyler, Ann. Phys. 158, 142 (1984); Nucl. Phys. B 250, 465 (1985).
- [37] J. Gasser and U. G. Meissner, Phys. Lett. B 258, 219 (1991); Nucl. Phys. B 357, 90 (1991).
- [38] J. V. Steele, H. Yamagishi, and I. Zahed, Nucl. Phys. A 615, 305 (1997).
- [39] T. N. Truong, Phys. Rev. Lett. 61, 2526 (1988); A. Dobado, M. J. Herrero, and T. N. Truong, Phys. Lett. B 235, 134 (1990); S. Willenbrock, Phys. Rev. D 43, 1710 (1991).
- [40] A. Dobado and J. R. Peláez, Phys. Lett. B 286, 136 (1992); A. Dobado and J. Morales, Phys. Rev. D 52, 2878 (1995).

- [41] G. F. Chew and S. Mandelstam, Phys. Rev. 119, 467 (1960); J. A. Oller and E. Oset, Phys. Rev. D 60, 074023 (1999); M. Albaladejo, J. A. Oller, and L. Roca, Phys. Rev. D 82, 094019 (2010).
- [42] T. N. Truong, Phys. Rev. Lett. 67, 2260 (1991); A. Dobado and J. R. Peláez, Phys. Rev. D 47, 4883 (1993); T. Hannah, Phys. Rev. D 55, 5613 (1997); A. Dobado and J. R. Peláez, Phys. Rev. D 56, 3057 (1997); M. Boggione and M. R. Pennington, Z. Phys. C 75, 113 (1997); J. Nieves, M. P. Valderrama, and E. R. Arriola, Phys. Rev. D 65, 036002 (2002).
- [43] B. S. Zou and D. V. Bugg, Phys. Rev. D 48, R3948 (1993); Phys. Rev. D 50, 591 (1994); F. Q. Wu, B. S. Zou, L. Li, and D. V. Bugg, Nucl. Phys. A 735, 111 (2004).
- [44] J. S. Borges, J. S. Barbosa, and V. Oguri, Phys. Lett. B 393, 413 (1997).
- [45] B. Ananthanarayan and P. Büttiker, Phys. Lett. B 415, 402 (1997); B. Ananthanarayan, Phys. Rev. D 58, 036002 (1998).
- [46] J. A. Oller and E. Oset, Nucl. Phys. A 620, 438 (1997); J. A. Oller, E. Oset, and J. R. Peláez, Phys. Rev. Lett. 80, 3452 (1998); Phys. Rev. D 59, 074001 (1999).
- [47] J. Nieves and E. R. Arriola, Phys. Lett. B 455, 30 (1999).
- [48] G. Janssen, B. C. Pearce, K. Holinde, and J. Speth, Phys. Rev. D 52, 2690 (1995).
- [49] B. A. Li, Phys. Rev. D 52, 5165 (1995).
- [50] Y. B. He, J. Hüfner, S. P. Klevansky, and P. Rehberg, Nucl. Phys. A 630, 719 (1998).
- [51] H. Chen, Phys. Rev. D 80, 034029 (2009).
- [52] R. García-Martín and B. Moussallam, Eur. Phys. J. C 70, 155 (2010).
- [53] I. V. Danilkin, L. I. R. Gil, and M. F. M. Lutz, Phys. Lett. B 703, 504 (2011).
- [54] N. N. Achasov and A. V. Kiselev, Phys. Rev. D 83, 054008 (2011).
- [55] M. Albaladejo, J. A. Oller, E. Oset, G. Rios, and L. Roca, JHEP 08, 071 (2012).

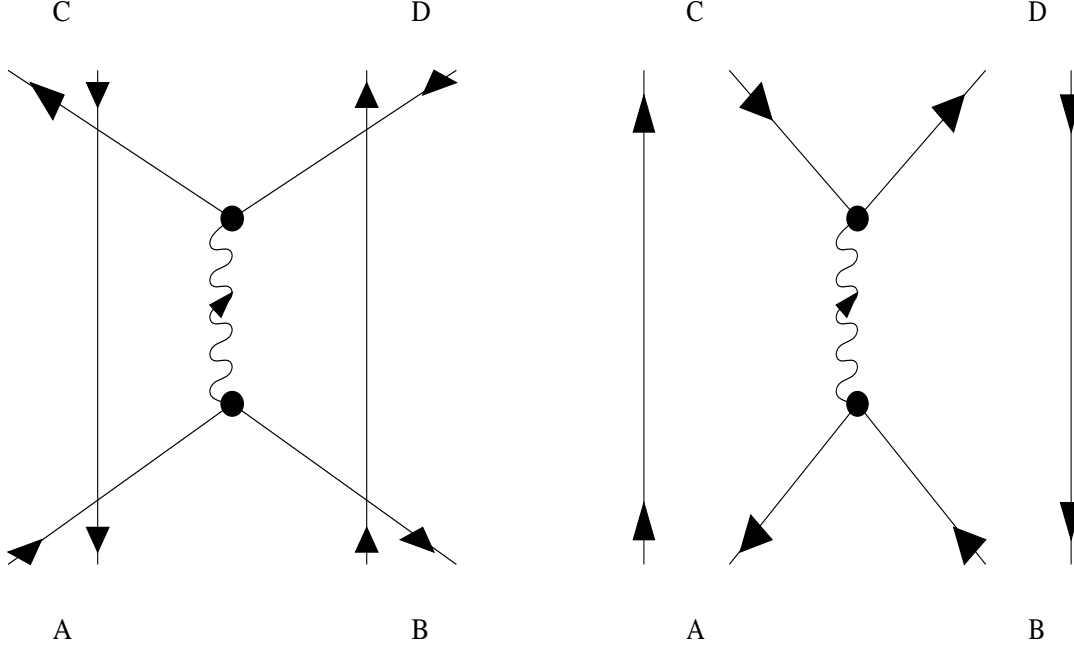


Figure 1: Left diagram with $q_1 + \bar{q}_2 \rightarrow q_3 + \bar{q}_4$ and right diagram with $\bar{q}_1 + q_2 \rightarrow q_3 + \bar{q}_4$ for $A + B \rightarrow C + D$. The vertical lines represent spectator quarks (antiquarks) of the mesons A, B, C, D .

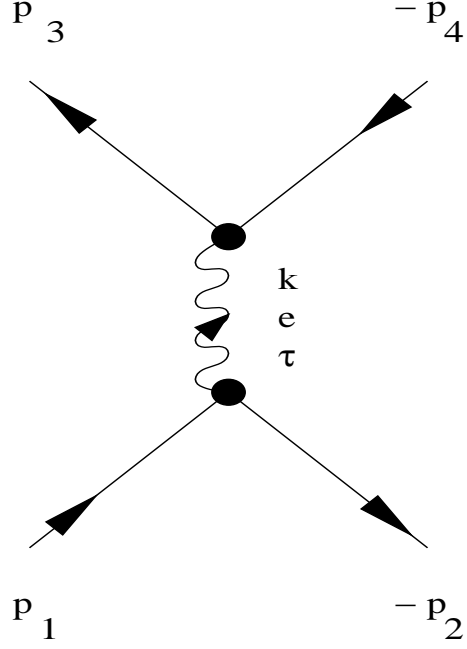


Figure 2: Quark-antiquark annihilation and creation: $q(p_1) + \bar{q}(-p_2) \rightarrow q'(p_3) + \bar{q}'(-p_4)$, where k denotes the gluon four-momentum, e its color index and τ its space-time index (cf. Eq. (39)).

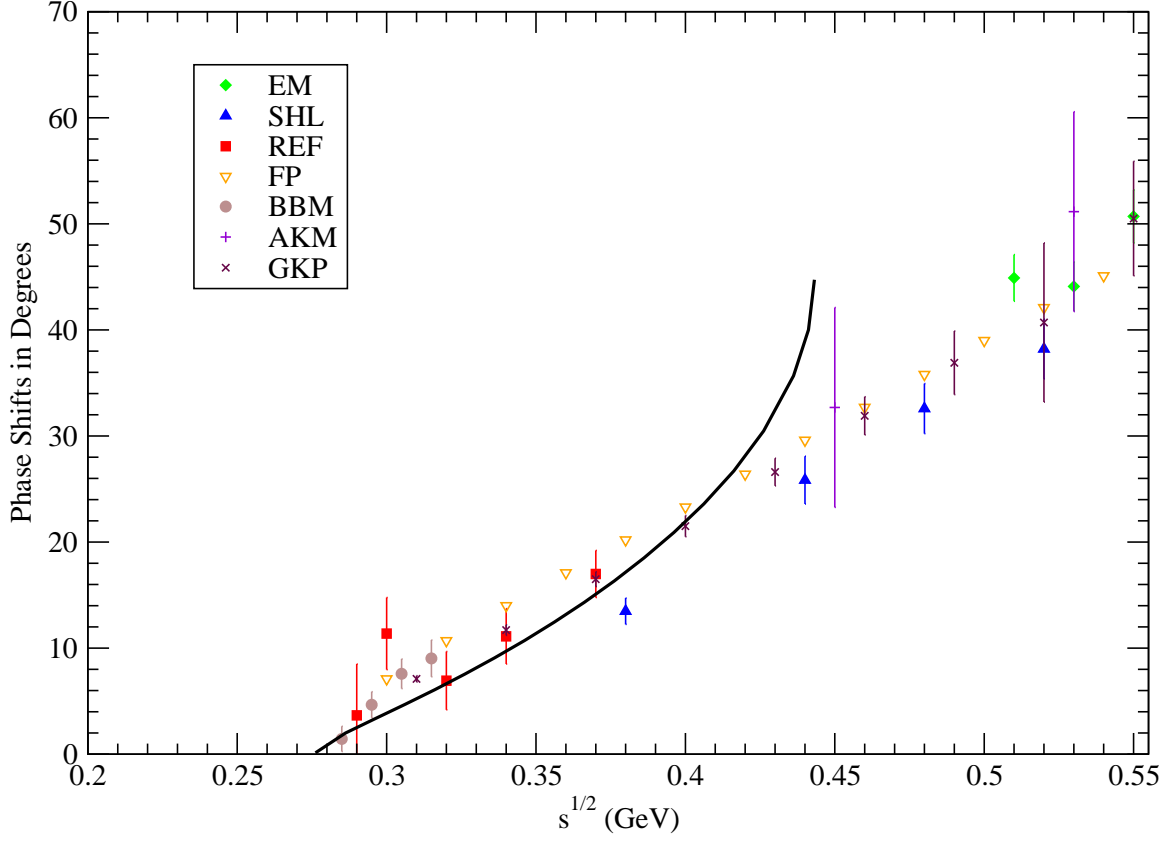


Figure 3: S -wave $I = 0$ elastic phase shifts for $\pi\pi$ scattering. The solid curve is the present theoretical result. Experimental data: \diamond , Ref. [29]; \triangle , Ref. [30]; \square , Ref. [31]; ∇ , Ref. [32]; \circ , Ref. [33]; $+$, Ref. [34]; \times , Ref. [35].

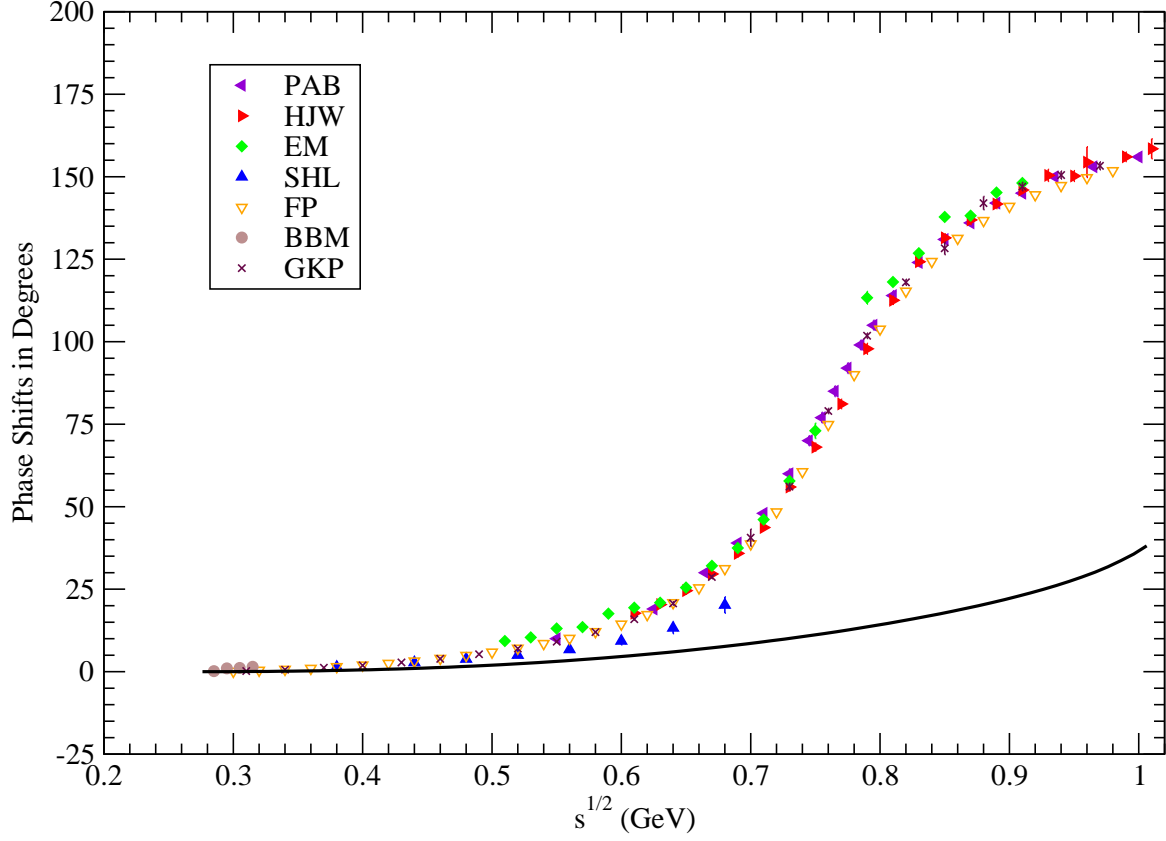


Figure 4: P -wave $I = 1$ elastic phase shifts for $\pi\pi$ scattering. The solid curve is the present theoretical result. Experimental data: \blacktriangleleft , Ref. [27]; \blacktriangleright , Ref. [28]; \blacklozenge , Ref. [29]; \blacktriangle , Ref. [30]; \blacktriangledown , Ref. [32]; \bigcirc , Ref. [33]; \times , Ref. [35].

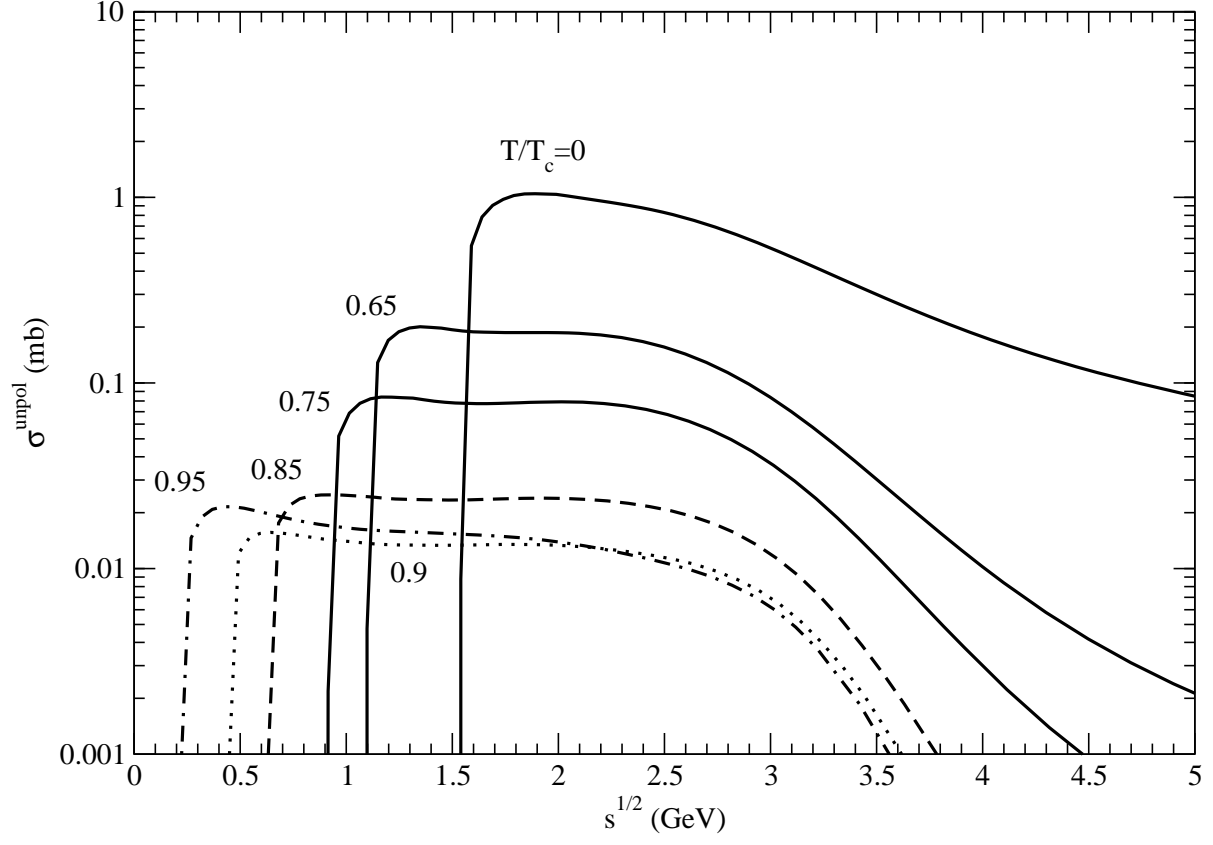


Figure 5: Cross sections for $\pi\pi \rightarrow \rho\rho$ for $I = 1$ at various temperatures.

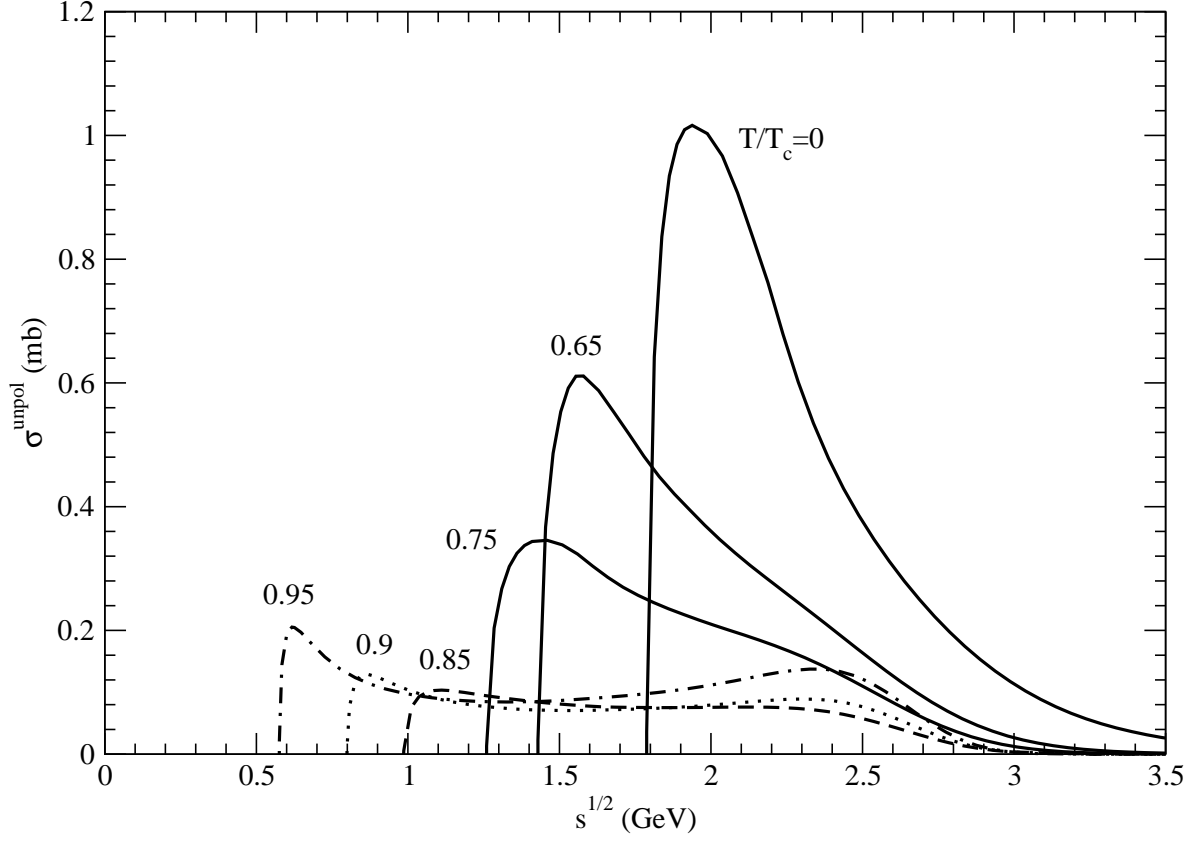


Figure 6: Cross sections for $K\bar{K} \rightarrow K^*\bar{K}^*$ for $I = 1$ at various temperatures.

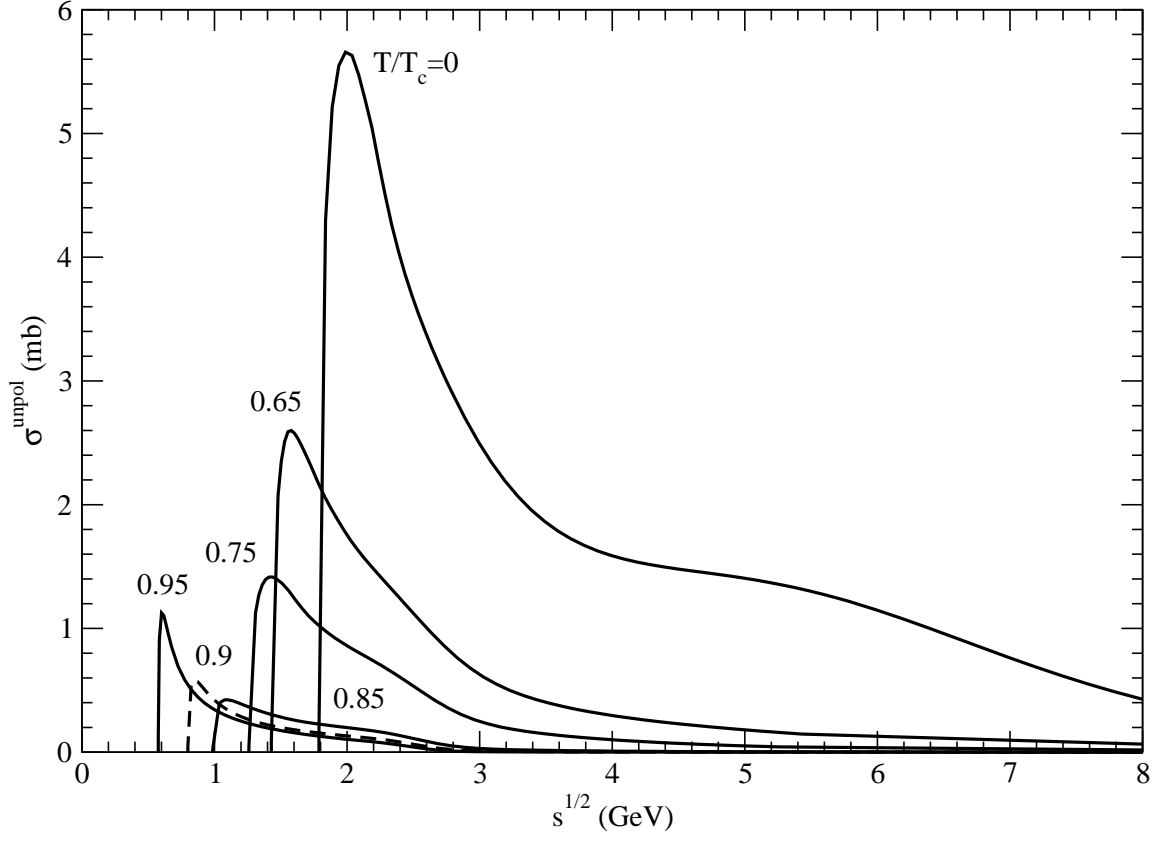


Figure 7: Cross sections for $K\bar{K} \rightarrow K^*\bar{K}^*$ for $I = 0$ at various temperatures.

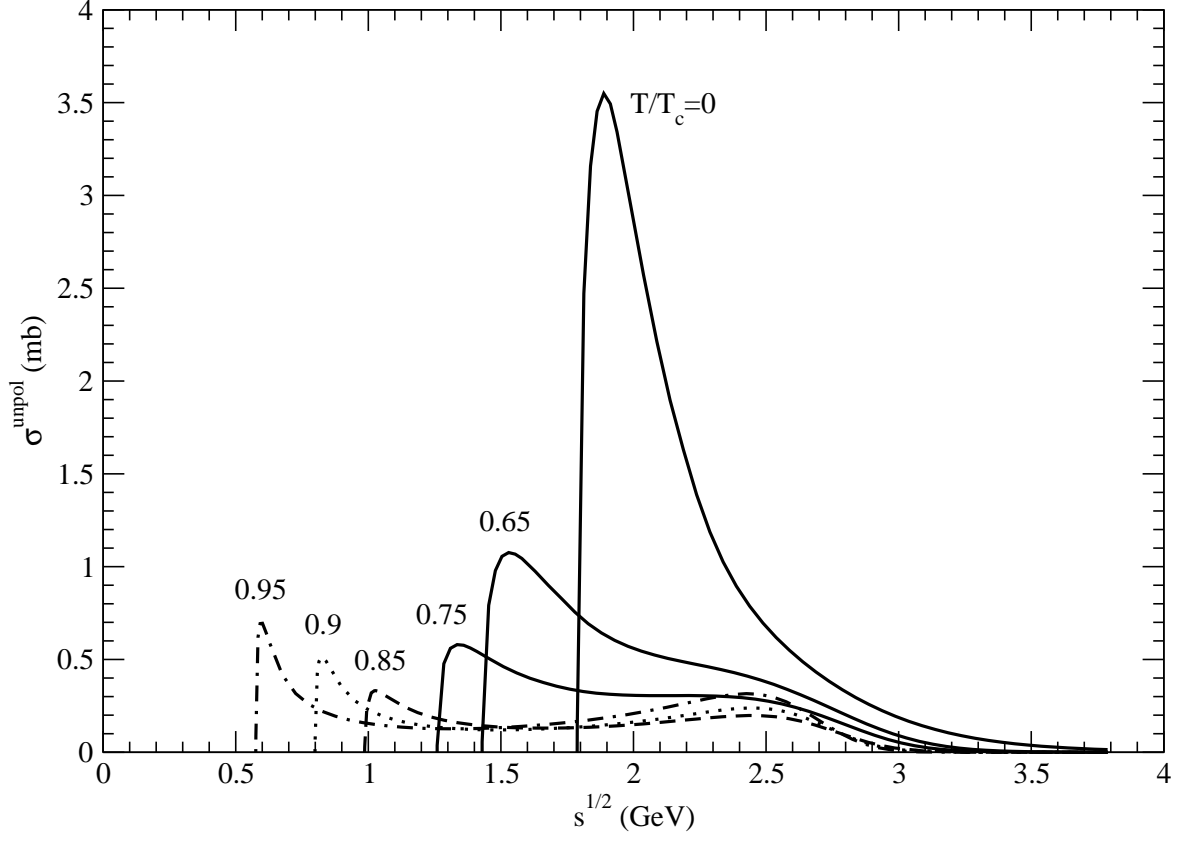


Figure 8: Cross sections for $K\bar{K}^* \rightarrow K^*\bar{K}^*$ for $I = 1$ at various temperatures.

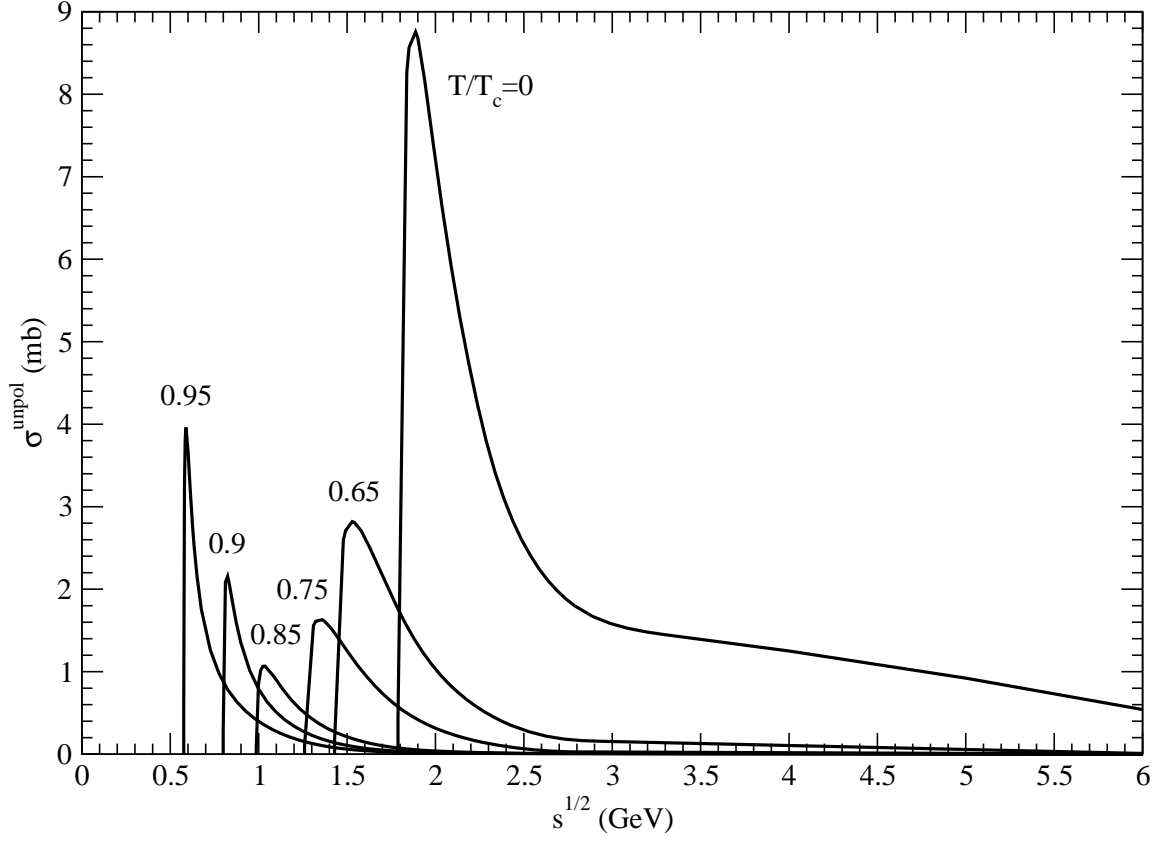


Figure 9: Cross sections for $K\bar{K}^* \rightarrow K^*\bar{K}^*$ for $I = 0$ at various temperatures.

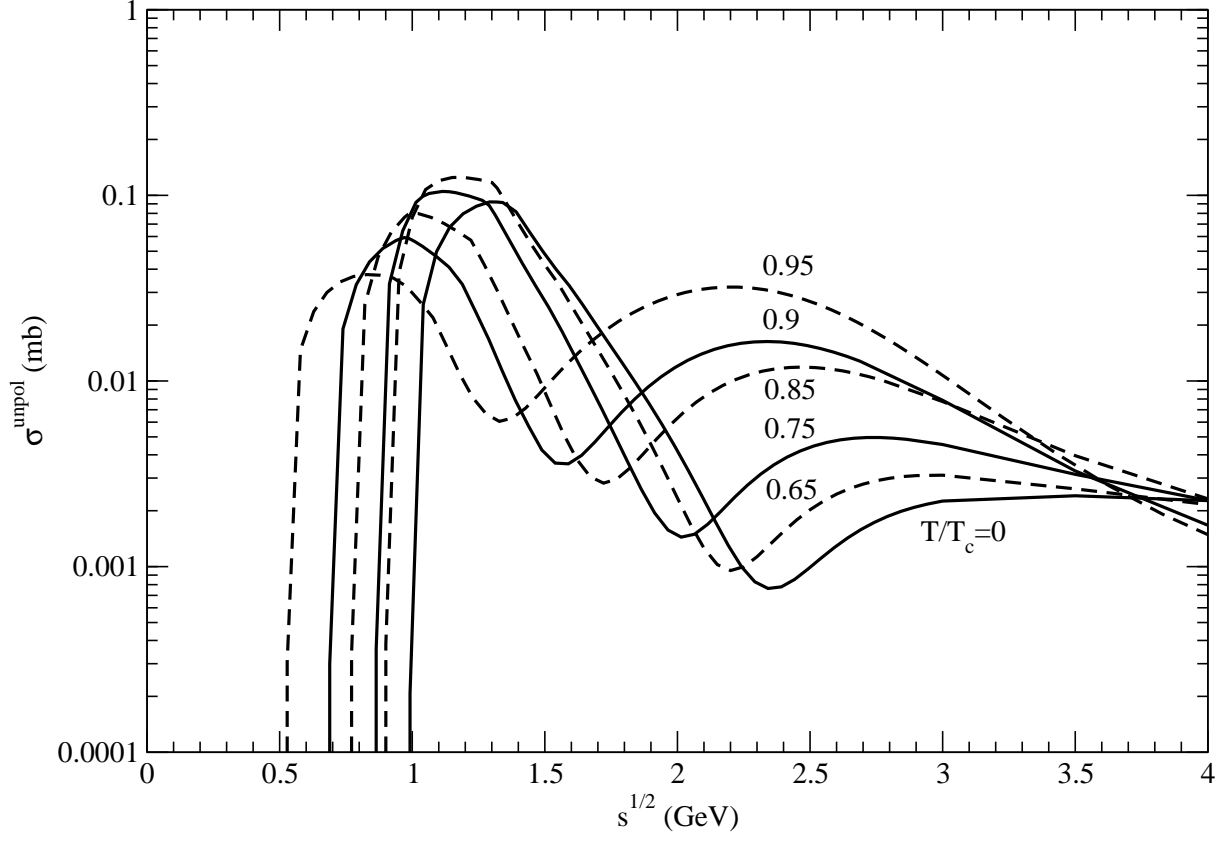


Figure 10: Cross sections for $\pi\pi \rightarrow K\bar{K}$ for $I = 1$ at various temperatures.

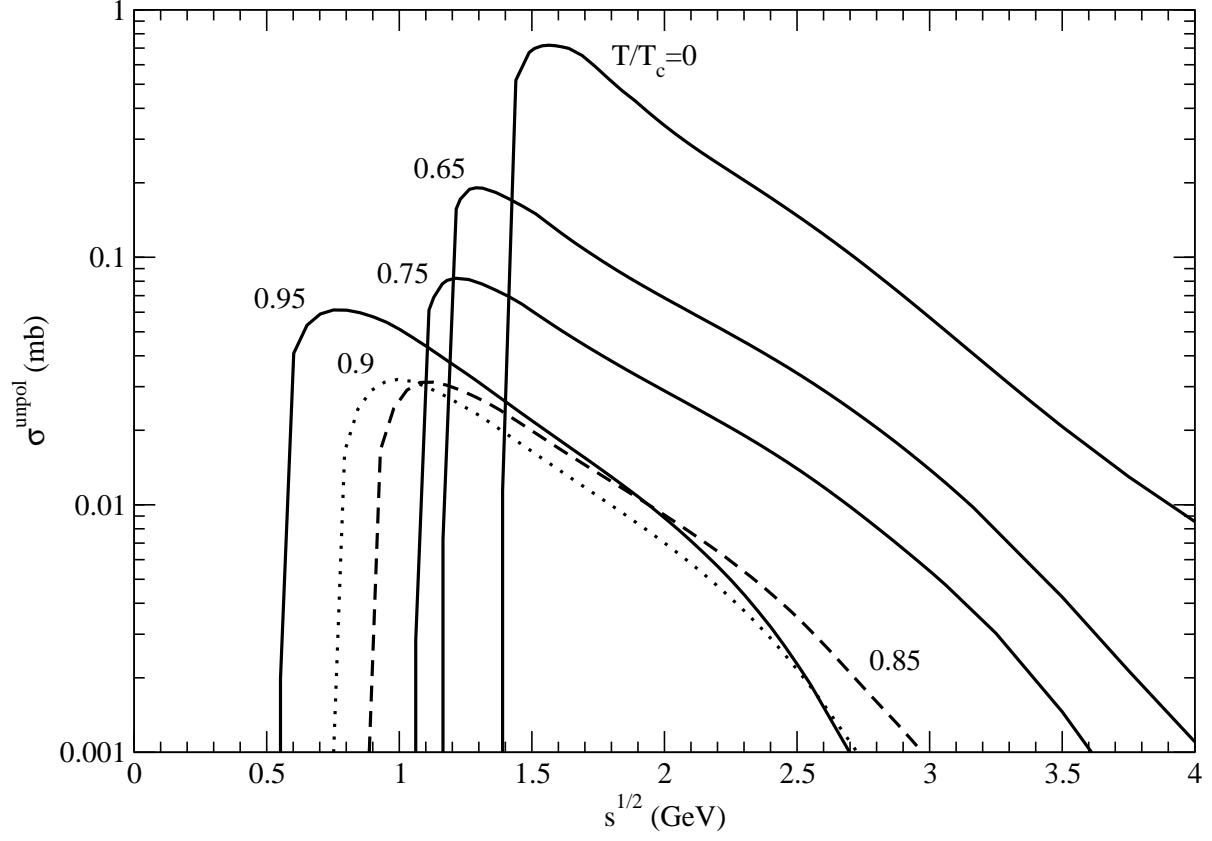


Figure 11: Cross sections for $\pi\rho \rightarrow K\bar{K}^*$ for $I = 1$ at various temperatures.

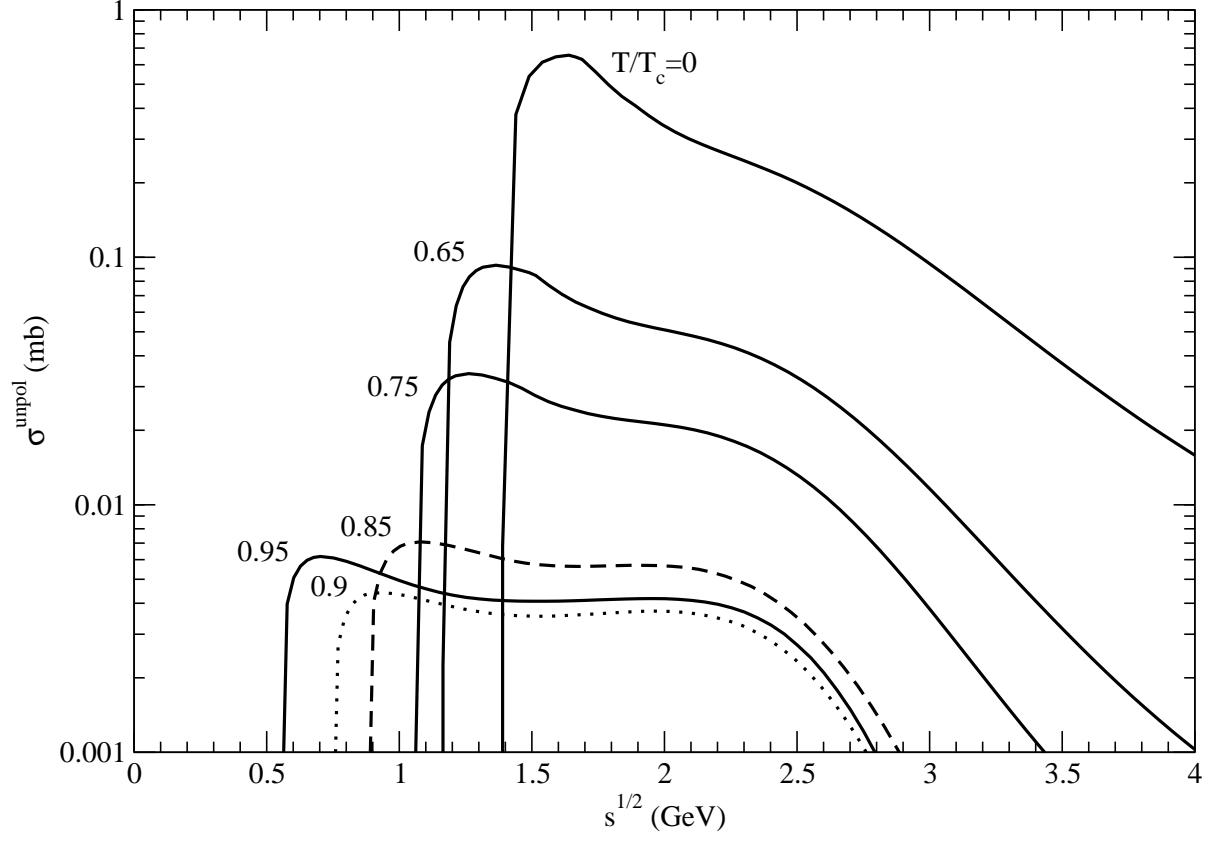


Figure 12: Cross sections for $\pi\rho \rightarrow K^*\bar{K}$ for $I = 1$ at various temperatures.

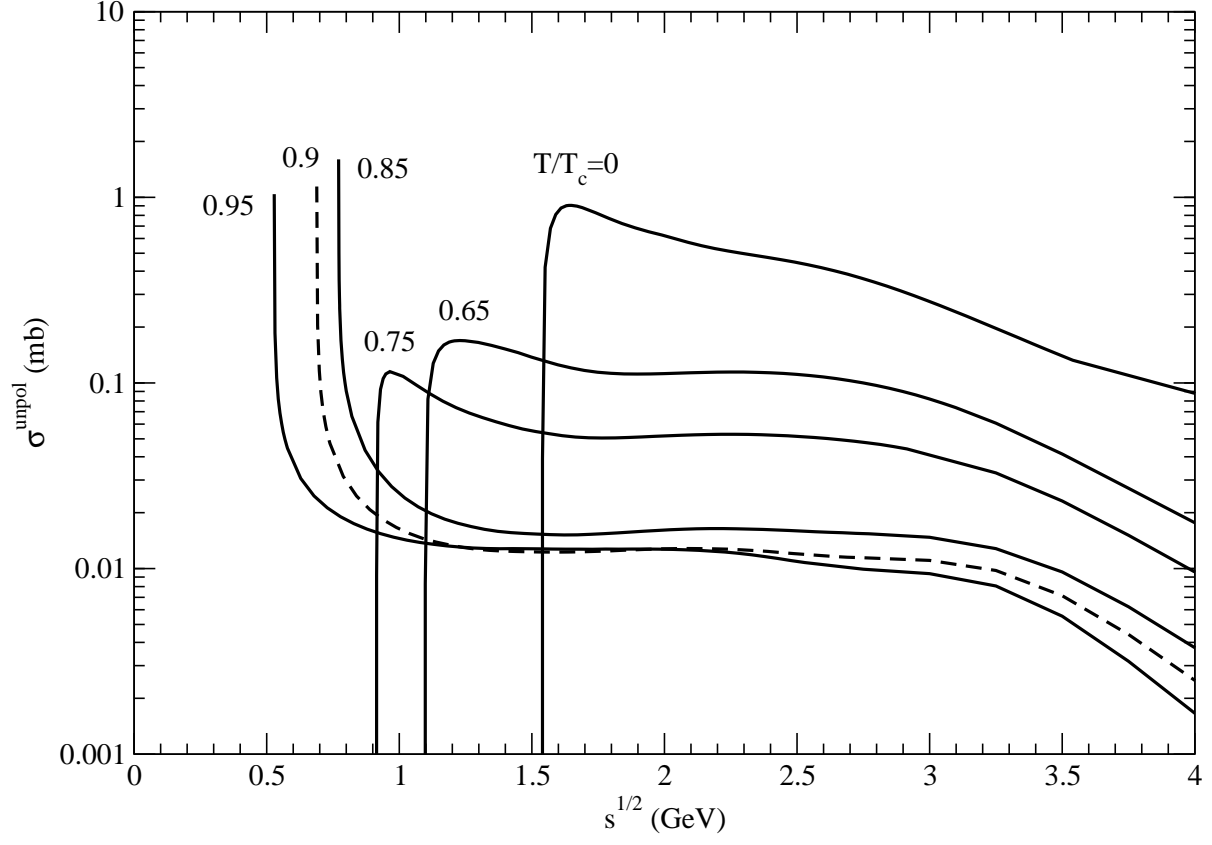


Figure 13: Cross sections for $K\bar{K} \rightarrow \rho\rho$ for $I = 1$ at various temperatures.

Table 1: Spin matrix elements of $\mathcal{M}_{a q_1 \bar{q}_2}$. The initial spin state is $\phi_{\text{iss}} = \chi_{S_A S_{A_z}} \chi_{S_B S_{B_z}}$, and the final spin state $\phi_{\text{fss}} = \chi_{S_C S_{C_z}} \chi_{S_D S_{D_z}}$. The second column corresponds to $S_A = S_B = S_C = S_D = 0$, the third to fifth columns correspond to $S_A = S_B = S_C = 0$, the sixth to eighth columns $S_A = S_B = S_D = 0$, and the ninth to eleventh columns $S_A = S_C = S_D = 0$.

S_{Az}	0	0	0	0	0	0	0	0	0	0
S_{Bz}	0	0	0	0	0	0	0	-1	0	1
S_{Cz}	0	0	0	0	-1	0	1	0	0	0
S_{Dz}	0	-1	0	1	0	0	0	0	0	0
$\phi_{\text{fss}}^+ \phi_{\text{iss}}$	$\frac{1}{2}$	0	0	0	0	0	0	0	0	0
$\phi_{\text{fss}}^+ \sigma_1(21) \phi_{\text{iss}}$	0	$-\frac{1}{2\sqrt{2}}$	0	$\frac{1}{2\sqrt{2}}$	$\frac{1}{2\sqrt{2}}$	0	$-\frac{1}{2\sqrt{2}}$	$-\frac{1}{2\sqrt{2}}$	0	$\frac{1}{2\sqrt{2}}$
$\phi_{\text{fss}}^+ \sigma_2(21) \phi_{\text{iss}}$	0	$\frac{1}{2\sqrt{2}}i$	0	$\frac{1}{2\sqrt{2}}i$	$\frac{1}{2\sqrt{2}}i$	0	$\frac{1}{2\sqrt{2}}i$	$-\frac{1}{2\sqrt{2}}i$	0	$-\frac{1}{2\sqrt{2}}i$
$\phi_{\text{fss}}^+ \sigma_3(21) \phi_{\text{iss}}$	0	0	$-\frac{1}{2}$	0	0	$\frac{1}{2}$	0	0	$-\frac{1}{2}$	0
$\phi_{\text{fss}}^+ \sigma_1(34) \phi_{\text{iss}}$	0	$-\frac{1}{2\sqrt{2}}$	0	$\frac{1}{2\sqrt{2}}$	$\frac{1}{2\sqrt{2}}$	0	$-\frac{1}{2\sqrt{2}}$	$-\frac{1}{2\sqrt{2}}$	0	$\frac{1}{2\sqrt{2}}$
$\phi_{\text{fss}}^+ \sigma_2(34) \phi_{\text{iss}}$	0	$\frac{1}{2\sqrt{2}}i$	0	$\frac{1}{2\sqrt{2}}i$	$\frac{1}{2\sqrt{2}}i$	0	$\frac{1}{2\sqrt{2}}i$	$-\frac{1}{2\sqrt{2}}i$	0	$-\frac{1}{2\sqrt{2}}i$
$\phi_{\text{fss}}^+ \sigma_3(34) \phi_{\text{iss}}$	0	0	$-\frac{1}{2}$	0	0	$\frac{1}{2}$	0	0	$-\frac{1}{2}$	0
$\phi_{\text{fss}}^+ \sigma_1(21) \sigma_1(34) \phi_{\text{iss}}$	$\frac{1}{2}$	0	0	0	0	0	0	0	0	0
$\phi_{\text{fss}}^+ \sigma_1(21) \sigma_2(34) \phi_{\text{iss}}$	0	0	$-\frac{1}{2}i$	0	0	$-\frac{1}{2}i$	0	0	$-\frac{1}{2}i$	0
$\phi_{\text{fss}}^+ \sigma_1(21) \sigma_3(34) \phi_{\text{iss}}$	0	$\frac{1}{2\sqrt{2}}$	0	$\frac{1}{2\sqrt{2}}$	$-\frac{1}{2\sqrt{2}}$	0	$-\frac{1}{2\sqrt{2}}$	$-\frac{1}{2\sqrt{2}}$	0	$-\frac{1}{2\sqrt{2}}$
$\phi_{\text{fss}}^+ \sigma_2(21) \sigma_1(34) \phi_{\text{iss}}$	0	0	$\frac{1}{2}i$	0	0	$\frac{1}{2}i$	0	0	$\frac{1}{2}i$	0
$\phi_{\text{fss}}^+ \sigma_2(21) \sigma_2(34) \phi_{\text{iss}}$	$\frac{1}{2}$	0	0	0	0	0	0	0	0	0
$\phi_{\text{fss}}^+ \sigma_2(21) \sigma_3(34) \phi_{\text{iss}}$	0	$-\frac{1}{2\sqrt{2}}i$	0	$\frac{1}{2\sqrt{2}}i$	$-\frac{1}{2\sqrt{2}}i$	0	$\frac{1}{2\sqrt{2}}i$	$-\frac{1}{2\sqrt{2}}i$	0	$\frac{1}{2\sqrt{2}}i$
$\phi_{\text{fss}}^+ \sigma_3(21) \sigma_1(34) \phi_{\text{iss}}$	0	$-\frac{1}{2\sqrt{2}}$	0	$-\frac{1}{2\sqrt{2}}$	$\frac{1}{2\sqrt{2}}$	0	$\frac{1}{2\sqrt{2}}$	$\frac{1}{2\sqrt{2}}$	0	$\frac{1}{2\sqrt{2}}$
$\phi_{\text{fss}}^+ \sigma_3(21) \sigma_2(34) \phi_{\text{iss}}$	0	$\frac{1}{2\sqrt{2}}i$	0	$-\frac{1}{2\sqrt{2}}i$	$\frac{1}{2\sqrt{2}}i$	0	$-\frac{1}{2\sqrt{2}}i$	$\frac{1}{2\sqrt{2}}i$	0	$-\frac{1}{2\sqrt{2}}i$
$\phi_{\text{fss}}^+ \sigma_3(21) \sigma_3(34) \phi_{\text{iss}}$	$\frac{1}{2}$	0	0	0	0	0	0	0	0	0

Table 2: Spin matrix elements of $\mathcal{M}_{aq_1\bar{q}_2}$ at $S_A = S_B = 0$ and $S_C = S_D = 1$. The initial spin state is $\phi_{\text{iss}} = \chi_{S_A S_{A_z}} \chi_{S_B S_{B_z}}$, and the final spin state $\phi_{\text{fss}} = \chi_{S_C S_{C_z}} \chi_{S_D S_{D_z}}$.

S_{Cz}	-1	-1	-1	0	0	0	1	1	1
S_{Dz}	-1	0	1	-1	0	1	-1	0	1
$\phi_{\text{fss}}^+ \phi_{\text{iss}}$	$-\frac{1}{2}$	0	0	0	$-\frac{1}{2}$	0	0	0	$-\frac{1}{2}$
$\phi_{\text{fss}}^+ \sigma_1(21) \phi_{\text{iss}}$	0	$\frac{1}{2\sqrt{2}}$	0	$\frac{1}{2\sqrt{2}}$	0	$\frac{1}{2\sqrt{2}}$	0	$\frac{1}{2\sqrt{2}}$	0
$\phi_{\text{fss}}^+ \sigma_2(21) \phi_{\text{iss}}$	0	$\frac{1}{2\sqrt{2}}i$	0	$-\frac{1}{2\sqrt{2}}i$	0	$\frac{1}{2\sqrt{2}}i$	0	$-\frac{1}{2\sqrt{2}}i$	0
$\phi_{\text{fss}}^+ \sigma_3(21) \phi_{\text{iss}}$	$-\frac{1}{2}$	0	0	0	0	0	0	0	$\frac{1}{2}$
$\phi_{\text{fss}}^+ \sigma_1(34) \phi_{\text{iss}}$	0	$-\frac{1}{2\sqrt{2}}$	0	$-\frac{1}{2\sqrt{2}}$	0	$-\frac{1}{2\sqrt{2}}$	0	$-\frac{1}{2\sqrt{2}}$	0
$\phi_{\text{fss}}^+ \sigma_2(34) \phi_{\text{iss}}$	0	$-\frac{1}{2\sqrt{2}}i$	0	$\frac{1}{2\sqrt{2}}i$	0	$-\frac{1}{2\sqrt{2}}i$	0	$\frac{1}{2\sqrt{2}}i$	0
$\phi_{\text{fss}}^+ \sigma_3(34) \phi_{\text{iss}}$	$\frac{1}{2}$	0	0	0	0	0	0	0	$-\frac{1}{2}$
$\phi_{\text{fss}}^+ \sigma_1(21) \sigma_1(34) \phi_{\text{iss}}$	0	0	$\frac{1}{2}$	0	$\frac{1}{2}$	0	$\frac{1}{2}$	0	0
$\phi_{\text{fss}}^+ \sigma_1(21) \sigma_2(34) \phi_{\text{iss}}$	0	0	$\frac{1}{2}i$	0	0	0	$-\frac{1}{2}i$	0	0
$\phi_{\text{fss}}^+ \sigma_1(21) \sigma_3(34) \phi_{\text{iss}}$	0	$-\frac{1}{2\sqrt{2}}$	0	$-\frac{1}{2\sqrt{2}}$	0	$\frac{1}{2\sqrt{2}}$	0	$\frac{1}{2\sqrt{2}}$	0
$\phi_{\text{fss}}^+ \sigma_2(21) \sigma_1(34) \phi_{\text{iss}}$	0	0	$\frac{1}{2}i$	0	0	0	$-\frac{1}{2}i$	0	0
$\phi_{\text{fss}}^+ \sigma_2(21) \sigma_2(34) \phi_{\text{iss}}$	0	0	$-\frac{1}{2}$	0	$\frac{1}{2}$	0	$-\frac{1}{2}$	0	0
$\phi_{\text{fss}}^+ \sigma_2(21) \sigma_3(34) \phi_{\text{iss}}$	0	$-\frac{1}{2\sqrt{2}}i$	0	$\frac{1}{2\sqrt{2}}i$	0	$\frac{1}{2\sqrt{2}}i$	0	$-\frac{1}{2\sqrt{2}}i$	0
$\phi_{\text{fss}}^+ \sigma_3(21) \sigma_1(34) \phi_{\text{iss}}$	0	$-\frac{1}{2\sqrt{2}}$	0	$-\frac{1}{2\sqrt{2}}$	0	$\frac{1}{2\sqrt{2}}$	0	$\frac{1}{2\sqrt{2}}$	0
$\phi_{\text{fss}}^+ \sigma_3(21) \sigma_2(34) \phi_{\text{iss}}$	0	$-\frac{1}{2\sqrt{2}}i$	0	$\frac{1}{2\sqrt{2}}i$	0	$\frac{1}{2\sqrt{2}}i$	0	$-\frac{1}{2\sqrt{2}}i$	0
$\phi_{\text{fss}}^+ \sigma_3(21) \sigma_3(34) \phi_{\text{iss}}$	$\frac{1}{2}$	0	0	0	$-\frac{1}{2}$	0	0	0	$\frac{1}{2}$

Table 3: The same as Table 2 except for $S_A = S_C = 0$ and $S_B = S_D = 1$.

S_{Bz}	-1	-1	-1	0	0	0	1	1	1
S_{Dz}	-1	0	1	-1	0	1	-1	0	1
$\phi_{\text{fss}}^+ \phi_{\text{iss}}$	$\frac{1}{2}$	0	0	0	$\frac{1}{2}$	0	0	0	$\frac{1}{2}$
$\phi_{\text{fss}}^+ \sigma_1(21) \phi_{\text{iss}}$	0	$\frac{1}{2\sqrt{2}}$	0	$\frac{1}{2\sqrt{2}}$	0	$\frac{1}{2\sqrt{2}}$	0	$\frac{1}{2\sqrt{2}}$	0
$\phi_{\text{fss}}^+ \sigma_2(21) \phi_{\text{iss}}$	0	$\frac{1}{2\sqrt{2}}i$	0	$-\frac{1}{2\sqrt{2}}i$	0	$\frac{1}{2\sqrt{2}}i$	0	$-\frac{1}{2\sqrt{2}}i$	0
$\phi_{\text{fss}}^+ \sigma_3(21) \phi_{\text{iss}}$	$-\frac{1}{2}$	0	0	0	0	0	0	0	$\frac{1}{2}$
$\phi_{\text{fss}}^+ \sigma_1(34) \phi_{\text{iss}}$	0	$\frac{1}{2\sqrt{2}}$	0	$\frac{1}{2\sqrt{2}}$	0	$\frac{1}{2\sqrt{2}}$	0	$\frac{1}{2\sqrt{2}}$	0
$\phi_{\text{fss}}^+ \sigma_2(34) \phi_{\text{iss}}$	0	$\frac{1}{2\sqrt{2}}i$	0	$-\frac{1}{2\sqrt{2}}i$	0	$\frac{1}{2\sqrt{2}}i$	0	$-\frac{1}{2\sqrt{2}}i$	0
$\phi_{\text{fss}}^+ \sigma_3(34) \phi_{\text{iss}}$	$-\frac{1}{2}$	0	0	0	0	0	0	0	$\frac{1}{2}$
$\phi_{\text{fss}}^+ \sigma_1(21) \sigma_1(34) \phi_{\text{iss}}$	$\frac{1}{2}$	0	0	0	$\frac{1}{2}$	0	0	0	$\frac{1}{2}$
$\phi_{\text{fss}}^+ \sigma_1(21) \sigma_2(34) \phi_{\text{iss}}$	$-\frac{1}{2}i$	0	0	0	0	0	0	0	$\frac{1}{2}i$
$\phi_{\text{fss}}^+ \sigma_1(21) \sigma_3(34) \phi_{\text{iss}}$	0	$\frac{1}{2\sqrt{2}}$	0	$-\frac{1}{2\sqrt{2}}$	0	$\frac{1}{2\sqrt{2}}$	0	$-\frac{1}{2\sqrt{2}}$	0
$\phi_{\text{fss}}^+ \sigma_2(21) \sigma_1(34) \phi_{\text{iss}}$	$\frac{1}{2}i$	0	0	0	0	0	0	0	$-\frac{1}{2}i$
$\phi_{\text{fss}}^+ \sigma_2(21) \sigma_2(34) \phi_{\text{iss}}$	$\frac{1}{2}$	0	0	0	$\frac{1}{2}$	0	0	0	$\frac{1}{2}$
$\phi_{\text{fss}}^+ \sigma_2(21) \sigma_3(34) \phi_{\text{iss}}$	0	$\frac{1}{2\sqrt{2}}i$	0	$\frac{1}{2\sqrt{2}}i$	0	$\frac{1}{2\sqrt{2}}i$	0	$\frac{1}{2\sqrt{2}}i$	0
$\phi_{\text{fss}}^+ \sigma_3(21) \sigma_1(34) \phi_{\text{iss}}$	0	$-\frac{1}{2\sqrt{2}}$	0	$\frac{1}{2\sqrt{2}}$	0	$-\frac{1}{2\sqrt{2}}$	0	$\frac{1}{2\sqrt{2}}$	0
$\phi_{\text{fss}}^+ \sigma_3(21) \sigma_2(34) \phi_{\text{iss}}$	0	$-\frac{1}{2\sqrt{2}}i$	0	$-\frac{1}{2\sqrt{2}}i$	0	$-\frac{1}{2\sqrt{2}}i$	0	$-\frac{1}{2\sqrt{2}}i$	0
$\phi_{\text{fss}}^+ \sigma_3(21) \sigma_3(34) \phi_{\text{iss}}$	$\frac{1}{2}$	0	0	0	$\frac{1}{2}$	0	0	0	$\frac{1}{2}$

Table 4: The same as Table 2 except for $S_A = S_D = 0$ and $S_B = S_C = 1$.

S_{Bz}	-1	-1	-1	0	0	0	1	1	1
S_{Cz}	-1	0	1	-1	0	1	-1	0	1
$\phi_{\text{fss}}^+ \phi_{\text{iss}}$	0	0	$\frac{1}{2}$	0	$-\frac{1}{2}$	0	$\frac{1}{2}$	0	0
$\phi_{\text{fss}}^+ \sigma_1(21) \phi_{\text{iss}}$	0	$-\frac{1}{2\sqrt{2}}$	0	$\frac{1}{2\sqrt{2}}$	0	$\frac{1}{2\sqrt{2}}$	0	$-\frac{1}{2\sqrt{2}}$	0
$\phi_{\text{fss}}^+ \sigma_2(21) \phi_{\text{iss}}$	0	$-\frac{1}{2\sqrt{2}}i$	0	$\frac{1}{2\sqrt{2}}i$	0	$-\frac{1}{2\sqrt{2}}i$	0	$\frac{1}{2\sqrt{2}}i$	0
$\phi_{\text{fss}}^+ \sigma_3(21) \phi_{\text{iss}}$	0	0	$-\frac{1}{2}$	0	0	0	$\frac{1}{2}$	0	0
$\phi_{\text{fss}}^+ \sigma_1(34) \phi_{\text{iss}}$	0	$\frac{1}{2\sqrt{2}}$	0	$-\frac{1}{2\sqrt{2}}$	0	$-\frac{1}{2\sqrt{2}}$	0	$\frac{1}{2\sqrt{2}}$	0
$\phi_{\text{fss}}^+ \sigma_2(34) \phi_{\text{iss}}$	0	$\frac{1}{2\sqrt{2}}i$	0	$-\frac{1}{2\sqrt{2}}i$	0	$\frac{1}{2\sqrt{2}}i$	0	$-\frac{1}{2\sqrt{2}}i$	0
$\phi_{\text{fss}}^+ \sigma_3(34) \phi_{\text{iss}}$	0	0	$\frac{1}{2}$	0	0	0	$-\frac{1}{2}$	0	0
$\phi_{\text{fss}}^+ \sigma_1(21) \sigma_1(34) \phi_{\text{iss}}$	$-\frac{1}{2}$	0	0	0	$\frac{1}{2}$	0	0	0	$-\frac{1}{2}$
$\phi_{\text{fss}}^+ \sigma_1(21) \sigma_2(34) \phi_{\text{iss}}$	$-\frac{1}{2}i$	0	0	0	0	0	0	0	$\frac{1}{2}i$
$\phi_{\text{fss}}^+ \sigma_1(21) \sigma_3(34) \phi_{\text{iss}}$	0	$-\frac{1}{2\sqrt{2}}$	0	$-\frac{1}{2\sqrt{2}}$	0	$\frac{1}{2\sqrt{2}}$	0	$\frac{1}{2\sqrt{2}}$	0
$\phi_{\text{fss}}^+ \sigma_2(21) \sigma_1(34) \phi_{\text{iss}}$	$-\frac{1}{2}i$	0	0	0	0	0	0	0	$\frac{1}{2}i$
$\phi_{\text{fss}}^+ \sigma_2(21) \sigma_2(34) \phi_{\text{iss}}$	$\frac{1}{2}$	0	0	0	$\frac{1}{2}$	0	0	0	$\frac{1}{2}$
$\phi_{\text{fss}}^+ \sigma_2(21) \sigma_3(34) \phi_{\text{iss}}$	0	$-\frac{1}{2\sqrt{2}}i$	0	$-\frac{1}{2\sqrt{2}}i$	0	$-\frac{1}{2\sqrt{2}}i$	0	$-\frac{1}{2\sqrt{2}}i$	0
$\phi_{\text{fss}}^+ \sigma_3(21) \sigma_1(34) \phi_{\text{iss}}$	0	$-\frac{1}{2\sqrt{2}}$	0	$-\frac{1}{2\sqrt{2}}$	0	$\frac{1}{2\sqrt{2}}$	0	$\frac{1}{2\sqrt{2}}$	0
$\phi_{\text{fss}}^+ \sigma_3(21) \sigma_2(34) \phi_{\text{iss}}$	0	$-\frac{1}{2\sqrt{2}}i$	0	$-\frac{1}{2\sqrt{2}}i$	0	$-\frac{1}{2\sqrt{2}}i$	0	$-\frac{1}{2\sqrt{2}}i$	0
$\phi_{\text{fss}}^+ \sigma_3(21) \sigma_3(34) \phi_{\text{iss}}$	0	0	$-\frac{1}{2}$	0	$-\frac{1}{2}$	0	$-\frac{1}{2}$	0	0

Table 5: The same as Table 2 except for $S_A = 0$, $S_{Cz} = 1$, and $S_B = S_C = S_D = 1$.

S_{Bz}	-1	-1	-1	0	0	0	1	1	1
S_{Dz}	-1	0	1	-1	0	1	-1	0	1
$\phi_{\text{fss}}^+ \phi_{\text{iss}}$	0	$-\frac{1}{2}$	0	0	0	$-\frac{1}{2}$	0	0	0
$\phi_{\text{fss}}^+ \sigma_1(21) \phi_{\text{iss}}$	0	0	0	0	$-\frac{1}{2\sqrt{2}}$	0	0	0	$-\frac{1}{\sqrt{2}}$
$\phi_{\text{fss}}^+ \sigma_2(21) \phi_{\text{iss}}$	0	0	0	0	$\frac{1}{2\sqrt{2}}i$	0	0	0	$\frac{1}{\sqrt{2}}i$
$\phi_{\text{fss}}^+ \sigma_3(21) \phi_{\text{iss}}$	0	$\frac{1}{2}$	0	0	0	$\frac{1}{2}$	0	0	0
$\phi_{\text{fss}}^+ \sigma_1(34) \phi_{\text{iss}}$	$-\frac{1}{\sqrt{2}}$	0	0	0	$-\frac{1}{2\sqrt{2}}$	0	0	0	0
$\phi_{\text{fss}}^+ \sigma_2(34) \phi_{\text{iss}}$	$\frac{1}{\sqrt{2}}i$	0	0	0	$\frac{1}{2\sqrt{2}}i$	0	0	0	0
$\phi_{\text{fss}}^+ \sigma_3(34) \phi_{\text{iss}}$	0	$-\frac{1}{2}$	0	0	0	$-\frac{1}{2}$	0	0	0
$\phi_{\text{fss}}^+ \sigma_1(21) \sigma_1(34) \phi_{\text{iss}}$	0	0	0	$-\frac{1}{2}$	0	0	0	$-\frac{1}{2}$	0
$\phi_{\text{fss}}^+ \sigma_1(21) \sigma_2(34) \phi_{\text{iss}}$	0	0	0	$\frac{1}{2}i$	0	0	0	$\frac{1}{2}i$	0
$\phi_{\text{fss}}^+ \sigma_1(21) \sigma_3(34) \phi_{\text{iss}}$	0	0	0	0	$-\frac{1}{2\sqrt{2}}$	0	0	0	$-\frac{1}{\sqrt{2}}$
$\phi_{\text{fss}}^+ \sigma_2(21) \sigma_1(34) \phi_{\text{iss}}$	0	0	0	$\frac{1}{2}i$	0	0	0	$\frac{1}{2}i$	0
$\phi_{\text{fss}}^+ \sigma_2(21) \sigma_2(34) \phi_{\text{iss}}$	0	0	0	$\frac{1}{2}$	0	0	0	$\frac{1}{2}$	0
$\phi_{\text{fss}}^+ \sigma_2(21) \sigma_3(34) \phi_{\text{iss}}$	0	0	0	0	$\frac{1}{2\sqrt{2}}i$	0	0	0	$\frac{1}{\sqrt{2}}i$
$\phi_{\text{fss}}^+ \sigma_3(21) \sigma_1(34) \phi_{\text{iss}}$	$\frac{1}{\sqrt{2}}$	0	0	0	$\frac{1}{2\sqrt{2}}$	0	0	0	0
$\phi_{\text{fss}}^+ \sigma_3(21) \sigma_2(34) \phi_{\text{iss}}$	$-\frac{1}{\sqrt{2}}i$	0	0	0	$-\frac{1}{2\sqrt{2}}i$	0	0	0	0
$\phi_{\text{fss}}^+ \sigma_3(21) \sigma_3(34) \phi_{\text{iss}}$	0	$\frac{1}{2}$	0	0	0	$\frac{1}{2}$	0	0	0

Table 6: The same as Table 2 except for $S_A = 0$, $S_{Cz} = 0$, and $S_B = S_C = S_D = 1$.

S_{Bz}	-1	-1	-1	0	0	0	1	1	1
S_{Dz}	-1	0	1	-1	0	1	-1	0	1
$\phi_{\text{fss}}^+ \phi_{\text{iss}}$	$-\frac{1}{2}$	0	0	0	0	0	0	0	$\frac{1}{2}$
$\phi_{\text{fss}}^+ \sigma_1(21) \phi_{\text{iss}}$	0	$\frac{1}{2\sqrt{2}}$	0	$-\frac{1}{2\sqrt{2}}$	0	$\frac{1}{2\sqrt{2}}$	0	$-\frac{1}{2\sqrt{2}}$	0
$\phi_{\text{fss}}^+ \sigma_2(21) \phi_{\text{iss}}$	0	$\frac{1}{2\sqrt{2}}i$	0	$\frac{1}{2\sqrt{2}}i$	0	$\frac{1}{2\sqrt{2}}i$	0	$\frac{1}{2\sqrt{2}}i$	0
$\phi_{\text{fss}}^+ \sigma_3(21) \phi_{\text{iss}}$	$\frac{1}{2}$	0	0	0	$\frac{1}{2}$	0	0	0	$\frac{1}{2}$
$\phi_{\text{fss}}^+ \sigma_1(34) \phi_{\text{iss}}$	0	$-\frac{1}{2\sqrt{2}}$	0	$\frac{1}{2\sqrt{2}}$	0	$-\frac{1}{2\sqrt{2}}$	0	$\frac{1}{2\sqrt{2}}$	0
$\phi_{\text{fss}}^+ \sigma_2(34) \phi_{\text{iss}}$	0	$-\frac{1}{2\sqrt{2}}i$	0	$-\frac{1}{2\sqrt{2}}i$	0	$-\frac{1}{2\sqrt{2}}i$	0	$-\frac{1}{2\sqrt{2}}i$	0
$\phi_{\text{fss}}^+ \sigma_3(34) \phi_{\text{iss}}$	$\frac{1}{2}$	0	0	0	$\frac{1}{2}$	0	0	0	$\frac{1}{2}$
$\phi_{\text{fss}}^+ \sigma_1(21) \sigma_1(34) \phi_{\text{iss}}$	$\frac{1}{2}$	0	0	0	0	0	0	0	$-\frac{1}{2}$
$\phi_{\text{fss}}^+ \sigma_1(21) \sigma_2(34) \phi_{\text{iss}}$	$-\frac{1}{2}i$	0	0	0	$-\frac{1}{2}i$	0	0	0	$-\frac{1}{2}i$
$\phi_{\text{fss}}^+ \sigma_1(21) \sigma_3(34) \phi_{\text{iss}}$	0	$\frac{1}{2\sqrt{2}}$	0	$\frac{1}{2\sqrt{2}}$	0	$\frac{1}{2\sqrt{2}}$	0	$\frac{1}{2\sqrt{2}}$	0
$\phi_{\text{fss}}^+ \sigma_2(21) \sigma_1(34) \phi_{\text{iss}}$	$\frac{1}{2}i$	0	0	0	$\frac{1}{2}i$	0	0	0	$\frac{1}{2}i$
$\phi_{\text{fss}}^+ \sigma_2(21) \sigma_2(34) \phi_{\text{iss}}$	$\frac{1}{2}$	0	0	0	0	0	0	0	$-\frac{1}{2}$
$\phi_{\text{fss}}^+ \sigma_2(21) \sigma_3(34) \phi_{\text{iss}}$	0	$\frac{1}{2\sqrt{2}}i$	0	$-\frac{1}{2\sqrt{2}}i$	0	$\frac{1}{2\sqrt{2}}i$	0	$-\frac{1}{2\sqrt{2}}i$	0
$\phi_{\text{fss}}^+ \sigma_3(21) \sigma_1(34) \phi_{\text{iss}}$	0	$\frac{1}{2\sqrt{2}}$	0	$\frac{1}{2\sqrt{2}}$	0	$\frac{1}{2\sqrt{2}}$	0	$\frac{1}{2\sqrt{2}}$	0
$\phi_{\text{fss}}^+ \sigma_3(21) \sigma_2(34) \phi_{\text{iss}}$	0	$\frac{1}{2\sqrt{2}}i$	0	$-\frac{1}{2\sqrt{2}}i$	0	$\frac{1}{2\sqrt{2}}i$	0	$-\frac{1}{2\sqrt{2}}i$	0
$\phi_{\text{fss}}^+ \sigma_3(21) \sigma_3(34) \phi_{\text{iss}}$	$-\frac{1}{2}$	0	0	0	0	0	0	0	$\frac{1}{2}$

Table 7: The same as Table 2 except for $S_A = 0$, $S_{Cz} = -1$, and $S_B = S_C = S_D = 1$.

S_{Bz}	-1	-1	-1	0	0	0	1	1	1
S_{Dz}	-1	0	1	-1	0	1	-1	0	1
$\phi_{\text{fss}}^+ \phi_{\text{iss}}$	0	0	0	$\frac{1}{2}$	0	0	0	$\frac{1}{2}$	0
$\phi_{\text{fss}}^+ \sigma_1(21) \phi_{\text{iss}}$	$\frac{1}{\sqrt{2}}$	0	0	0	$\frac{1}{2\sqrt{2}}$	0	0	0	0
$\phi_{\text{fss}}^+ \sigma_2(21) \phi_{\text{iss}}$	$\frac{1}{\sqrt{2}}i$	0	0	0	$\frac{1}{2\sqrt{2}}i$	0	0	0	0
$\phi_{\text{fss}}^+ \sigma_3(21) \phi_{\text{iss}}$	0	0	0	$\frac{1}{2}$	0	0	0	$\frac{1}{2}$	0
$\phi_{\text{fss}}^+ \sigma_1(34) \phi_{\text{iss}}$	0	0	0	0	$\frac{1}{2\sqrt{2}}$	0	0	0	$\frac{1}{\sqrt{2}}$
$\phi_{\text{fss}}^+ \sigma_2(34) \phi_{\text{iss}}$	0	0	0	0	$\frac{1}{2\sqrt{2}}i$	0	0	0	$\frac{1}{\sqrt{2}}i$
$\phi_{\text{fss}}^+ \sigma_3(34) \phi_{\text{iss}}$	0	0	0	$-\frac{1}{2}$	0	0	0	$-\frac{1}{2}$	0
$\phi_{\text{fss}}^+ \sigma_1(21) \sigma_1(34) \phi_{\text{iss}}$	0	$\frac{1}{2}$	0	0	0	$\frac{1}{2}$	0	0	0
$\phi_{\text{fss}}^+ \sigma_1(21) \sigma_2(34) \phi_{\text{iss}}$	0	$\frac{1}{2}i$	0	0	0	$\frac{1}{2}i$	0	0	0
$\phi_{\text{fss}}^+ \sigma_1(21) \sigma_3(34) \phi_{\text{iss}}$	$-\frac{1}{\sqrt{2}}$	0	0	0	$-\frac{1}{2\sqrt{2}}$	0	0	0	0
$\phi_{\text{fss}}^+ \sigma_2(21) \sigma_1(34) \phi_{\text{iss}}$	0	$\frac{1}{2}i$	0	0	0	$\frac{1}{2}i$	0	0	0
$\phi_{\text{fss}}^+ \sigma_2(21) \sigma_2(34) \phi_{\text{iss}}$	0	$-\frac{1}{2}$	0	0	0	$-\frac{1}{2}$	0	0	0
$\phi_{\text{fss}}^+ \sigma_2(21) \sigma_3(34) \phi_{\text{iss}}$	$-\frac{1}{\sqrt{2}}i$	0	0	0	$-\frac{1}{2\sqrt{2}}i$	0	0	0	0
$\phi_{\text{fss}}^+ \sigma_3(21) \sigma_1(34) \phi_{\text{iss}}$	0	0	0	0	$\frac{1}{2\sqrt{2}}$	0	0	0	$\frac{1}{\sqrt{2}}$
$\phi_{\text{fss}}^+ \sigma_3(21) \sigma_2(34) \phi_{\text{iss}}$	0	0	0	0	$\frac{1}{2\sqrt{2}}i$	0	0	0	$\frac{1}{\sqrt{2}}i$
$\phi_{\text{fss}}^+ \sigma_3(21) \sigma_3(34) \phi_{\text{iss}}$	0	0	0	$-\frac{1}{2}$	0	0	0	$-\frac{1}{2}$	0

Table 8: The same as Table 2 except for $S_A = S_B = 1$ and $S_C = S_D = 0$.

S_{Az}	-1	-1	-1	0	0	0	1	1	1
S_{Bz}	-1	0	1	-1	0	1	-1	0	1
$\phi_{\text{fss}}^+ \phi_{\text{iss}}$	$-\frac{1}{2}$	0	0	0	$-\frac{1}{2}$	0	0	0	$-\frac{1}{2}$
$\phi_{\text{fss}}^+ \sigma_1(21) \phi_{\text{iss}}$	0	$-\frac{1}{2\sqrt{2}}$	0	$-\frac{1}{2\sqrt{2}}$	0	$-\frac{1}{2\sqrt{2}}$	0	$-\frac{1}{2\sqrt{2}}$	0
$\phi_{\text{fss}}^+ \sigma_2(21) \phi_{\text{iss}}$	0	$\frac{1}{2\sqrt{2}}i$	0	$-\frac{1}{2\sqrt{2}}i$	0	$\frac{1}{2\sqrt{2}}i$	0	$-\frac{1}{2\sqrt{2}}i$	0
$\phi_{\text{fss}}^+ \sigma_3(21) \phi_{\text{iss}}$	$\frac{1}{2}$	0	0	0	0	0	0	0	$-\frac{1}{2}$
$\phi_{\text{fss}}^+ \sigma_1(34) \phi_{\text{iss}}$	0	$\frac{1}{2\sqrt{2}}$	0	$\frac{1}{2\sqrt{2}}$	0	$\frac{1}{2\sqrt{2}}$	0	$\frac{1}{2\sqrt{2}}$	0
$\phi_{\text{fss}}^+ \sigma_2(34) \phi_{\text{iss}}$	0	$-\frac{1}{2\sqrt{2}}i$	0	$\frac{1}{2\sqrt{2}}i$	0	$-\frac{1}{2\sqrt{2}}i$	0	$\frac{1}{2\sqrt{2}}i$	0
$\phi_{\text{fss}}^+ \sigma_3(34) \phi_{\text{iss}}$	$-\frac{1}{2}$	0	0	0	0	0	0	0	$\frac{1}{2}$
$\phi_{\text{fss}}^+ \sigma_1(21) \sigma_1(34) \phi_{\text{iss}}$	0	0	$\frac{1}{2}$	0	$\frac{1}{2}$	0	$\frac{1}{2}$	0	0
$\phi_{\text{fss}}^+ \sigma_1(21) \sigma_2(34) \phi_{\text{iss}}$	0	0	$-\frac{1}{2}i$	0	0	0	$\frac{1}{2}i$	0	0
$\phi_{\text{fss}}^+ \sigma_1(21) \sigma_3(34) \phi_{\text{iss}}$	0	$-\frac{1}{2\sqrt{2}}$	0	$-\frac{1}{2\sqrt{2}}$	0	$\frac{1}{2\sqrt{2}}$	0	$\frac{1}{2\sqrt{2}}$	0
$\phi_{\text{fss}}^+ \sigma_2(21) \sigma_1(34) \phi_{\text{iss}}$	0	0	$-\frac{1}{2}i$	0	0	0	$\frac{1}{2}i$	0	0
$\phi_{\text{fss}}^+ \sigma_2(21) \sigma_2(34) \phi_{\text{iss}}$	0	0	$-\frac{1}{2}$	0	$\frac{1}{2}$	0	$-\frac{1}{2}$	0	0
$\phi_{\text{fss}}^+ \sigma_2(21) \sigma_3(34) \phi_{\text{iss}}$	0	$\frac{1}{2\sqrt{2}}i$	0	$-\frac{1}{2\sqrt{2}}i$	0	$-\frac{1}{2\sqrt{2}}i$	0	$\frac{1}{2\sqrt{2}}i$	0
$\phi_{\text{fss}}^+ \sigma_3(21) \sigma_1(34) \phi_{\text{iss}}$	0	$-\frac{1}{2\sqrt{2}}$	0	$-\frac{1}{2\sqrt{2}}$	0	$\frac{1}{2\sqrt{2}}$	0	$\frac{1}{2\sqrt{2}}$	0
$\phi_{\text{fss}}^+ \sigma_3(21) \sigma_2(34) \phi_{\text{iss}}$	0	$\frac{1}{2\sqrt{2}}i$	0	$-\frac{1}{2\sqrt{2}}i$	0	$-\frac{1}{2\sqrt{2}}i$	0	$\frac{1}{2\sqrt{2}}i$	0
$\phi_{\text{fss}}^+ \sigma_3(21) \sigma_3(34) \phi_{\text{iss}}$	$\frac{1}{2}$	0	0	0	$-\frac{1}{2}$	0	0	0	$\frac{1}{2}$

Table 9: The same as Table 2 except for $S_C = 0$, $S_{Az} = 1$, and $S_A = S_B = S_D = 1$.

S_{Bz}	-1	-1	-1	0	0	0	1	1	1
S_{Dz}	-1	0	1	-1	0	1	-1	0	1
$\phi_{\text{fss}}^+ \phi_{\text{iss}}$	0	0	0	$-\frac{1}{2}$	0	0	0	$-\frac{1}{2}$	0
$\phi_{\text{fss}}^+ \sigma_1(21) \phi_{\text{iss}}$	$-\frac{1}{\sqrt{2}}$	0	0	0	$-\frac{1}{2\sqrt{2}}$	0	0	0	0
$\phi_{\text{fss}}^+ \sigma_2(21) \phi_{\text{iss}}$	$-\frac{1}{\sqrt{2}}i$	0	0	0	$-\frac{1}{2\sqrt{2}}i$	0	0	0	0
$\phi_{\text{fss}}^+ \sigma_3(21) \phi_{\text{iss}}$	0	0	0	$-\frac{1}{2}$	0	0	0	$-\frac{1}{2}$	0
$\phi_{\text{fss}}^+ \sigma_1(34) \phi_{\text{iss}}$	0	0	0	0	$-\frac{1}{2\sqrt{2}}$	0	0	0	$-\frac{1}{\sqrt{2}}$
$\phi_{\text{fss}}^+ \sigma_2(34) \phi_{\text{iss}}$	0	0	0	0	$-\frac{1}{2\sqrt{2}}i$	0	0	0	$-\frac{1}{\sqrt{2}}i$
$\phi_{\text{fss}}^+ \sigma_3(34) \phi_{\text{iss}}$	0	0	0	$\frac{1}{2}$	0	0	0	$\frac{1}{2}$	0
$\phi_{\text{fss}}^+ \sigma_1(21) \sigma_1(34) \phi_{\text{iss}}$	0	$-\frac{1}{2}$	0	0	0	$-\frac{1}{2}$	0	0	0
$\phi_{\text{fss}}^+ \sigma_1(21) \sigma_2(34) \phi_{\text{iss}}$	0	$-\frac{1}{2}i$	0	0	0	$-\frac{1}{2}i$	0	0	0
$\phi_{\text{fss}}^+ \sigma_1(21) \sigma_3(34) \phi_{\text{iss}}$	$\frac{1}{\sqrt{2}}$	0	0	0	$\frac{1}{2\sqrt{2}}$	0	0	0	0
$\phi_{\text{fss}}^+ \sigma_2(21) \sigma_1(34) \phi_{\text{iss}}$	0	$-\frac{1}{2}i$	0	0	0	$-\frac{1}{2}i$	0	0	0
$\phi_{\text{fss}}^+ \sigma_2(21) \sigma_2(34) \phi_{\text{iss}}$	0	$\frac{1}{2}$	0	0	0	$\frac{1}{2}$	0	0	0
$\phi_{\text{fss}}^+ \sigma_2(21) \sigma_3(34) \phi_{\text{iss}}$	$\frac{1}{\sqrt{2}}i$	0	0	0	$\frac{1}{2\sqrt{2}}i$	0	0	0	0
$\phi_{\text{fss}}^+ \sigma_3(21) \sigma_1(34) \phi_{\text{iss}}$	0	0	0	0	$-\frac{1}{2\sqrt{2}}$	0	0	0	$-\frac{1}{\sqrt{2}}$
$\phi_{\text{fss}}^+ \sigma_3(21) \sigma_2(34) \phi_{\text{iss}}$	0	0	0	0	$-\frac{1}{2\sqrt{2}}i$	0	0	0	$-\frac{1}{\sqrt{2}}i$
$\phi_{\text{fss}}^+ \sigma_3(21) \sigma_3(34) \phi_{\text{iss}}$	0	0	0	$\frac{1}{2}$	0	0	0	$\frac{1}{2}$	0

Table 10: The same as Table 2 except for $S_C = 0$, $S_{Az} = 0$, and $S_A = S_B = S_D = 1$.

S_{Bz}	-1	-1	-1	0	0	0	1	1	1
S_{Dz}	-1	0	1	-1	0	1	-1	0	1
$\phi_{\text{fss}}^+ \phi_{\text{iss}}$	$-\frac{1}{2}$	0	0	0	0	0	0	0	$\frac{1}{2}$
$\phi_{\text{fss}}^+ \sigma_1(21) \phi_{\text{iss}}$	0	$\frac{1}{2\sqrt{2}}$	0	$-\frac{1}{2\sqrt{2}}$	0	$\frac{1}{2\sqrt{2}}$	0	$-\frac{1}{2\sqrt{2}}$	0
$\phi_{\text{fss}}^+ \sigma_2(21) \phi_{\text{iss}}$	0	$\frac{1}{2\sqrt{2}}i$	0	$\frac{1}{2\sqrt{2}}i$	0	$\frac{1}{2\sqrt{2}}i$	0	$\frac{1}{2\sqrt{2}}i$	0
$\phi_{\text{fss}}^+ \sigma_3(21) \phi_{\text{iss}}$	$\frac{1}{2}$	0	0	0	$\frac{1}{2}$	0	0	0	$\frac{1}{2}$
$\phi_{\text{fss}}^+ \sigma_1(34) \phi_{\text{iss}}$	0	$-\frac{1}{2\sqrt{2}}$	0	$\frac{1}{2\sqrt{2}}$	0	$-\frac{1}{2\sqrt{2}}$	0	$\frac{1}{2\sqrt{2}}$	0
$\phi_{\text{fss}}^+ \sigma_2(34) \phi_{\text{iss}}$	0	$-\frac{1}{2\sqrt{2}}i$	0	$-\frac{1}{2\sqrt{2}}i$	0	$-\frac{1}{2\sqrt{2}}i$	0	$-\frac{1}{2\sqrt{2}}i$	0
$\phi_{\text{fss}}^+ \sigma_3(34) \phi_{\text{iss}}$	$\frac{1}{2}$	0	0	0	$\frac{1}{2}$	0	0	0	$\frac{1}{2}$
$\phi_{\text{fss}}^+ \sigma_1(21) \sigma_1(34) \phi_{\text{iss}}$	$\frac{1}{2}$	0	0	0	0	0	0	0	$-\frac{1}{2}$
$\phi_{\text{fss}}^+ \sigma_1(21) \sigma_2(34) \phi_{\text{iss}}$	$-\frac{1}{2}i$	0	0	0	$-\frac{1}{2}i$	0	0	0	$-\frac{1}{2}i$
$\phi_{\text{fss}}^+ \sigma_1(21) \sigma_3(34) \phi_{\text{iss}}$	0	$\frac{1}{2\sqrt{2}}$	0	$\frac{1}{2\sqrt{2}}$	0	$\frac{1}{2\sqrt{2}}$	0	$\frac{1}{2\sqrt{2}}$	0
$\phi_{\text{fss}}^+ \sigma_2(21) \sigma_1(34) \phi_{\text{iss}}$	$\frac{1}{2}i$	0	0	0	$\frac{1}{2}i$	0	0	0	$\frac{1}{2}i$
$\phi_{\text{fss}}^+ \sigma_2(21) \sigma_2(34) \phi_{\text{iss}}$	$\frac{1}{2}$	0	0	0	0	0	0	0	$-\frac{1}{2}$
$\phi_{\text{fss}}^+ \sigma_2(21) \sigma_3(34) \phi_{\text{iss}}$	0	$\frac{1}{2\sqrt{2}}i$	0	$-\frac{1}{2\sqrt{2}}i$	0	$\frac{1}{2\sqrt{2}}i$	0	$-\frac{1}{2\sqrt{2}}i$	0
$\phi_{\text{fss}}^+ \sigma_3(21) \sigma_1(34) \phi_{\text{iss}}$	0	$\frac{1}{2\sqrt{2}}$	0	$\frac{1}{2\sqrt{2}}$	0	$\frac{1}{2\sqrt{2}}$	0	$\frac{1}{2\sqrt{2}}$	0
$\phi_{\text{fss}}^+ \sigma_3(21) \sigma_2(34) \phi_{\text{iss}}$	0	$\frac{1}{2\sqrt{2}}i$	0	$-\frac{1}{2\sqrt{2}}i$	0	$\frac{1}{2\sqrt{2}}i$	0	$-\frac{1}{2\sqrt{2}}i$	0
$\phi_{\text{fss}}^+ \sigma_3(21) \sigma_3(34) \phi_{\text{iss}}$	$-\frac{1}{2}$	0	0	0	0	0	0	0	$\frac{1}{2}$

Table 11: The same as Table 2 except for $S_C = 0$, $S_{Az} = -1$, and $S_A = S_B = S_D = 1$.

S_{Bz}	-1	-1	-1	0	0	0	1	1	1
S_{Dz}	-1	0	1	-1	0	1	-1	0	1
$\phi_{\text{fss}}^+ \phi_{\text{iss}}$	0	$\frac{1}{2}$	0	0	0	$\frac{1}{2}$	0	0	0
$\phi_{\text{fss}}^+ \sigma_1(21) \phi_{\text{iss}}$	0	0	0	0	$\frac{1}{2\sqrt{2}}$	0	0	0	$\frac{1}{\sqrt{2}}$
$\phi_{\text{fss}}^+ \sigma_2(21) \phi_{\text{iss}}$	0	0	0	0	$-\frac{1}{2\sqrt{2}}i$	0	0	0	$-\frac{1}{\sqrt{2}}i$
$\phi_{\text{fss}}^+ \sigma_3(21) \phi_{\text{iss}}$	0	$-\frac{1}{2}$	0	0	0	$-\frac{1}{2}$	0	0	0
$\phi_{\text{fss}}^+ \sigma_1(34) \phi_{\text{iss}}$	$\frac{1}{\sqrt{2}}$	0	0	0	$\frac{1}{2\sqrt{2}}$	0	0	0	0
$\phi_{\text{fss}}^+ \sigma_2(34) \phi_{\text{iss}}$	$-\frac{1}{\sqrt{2}}i$	0	0	0	$-\frac{1}{2\sqrt{2}}i$	0	0	0	0
$\phi_{\text{fss}}^+ \sigma_3(34) \phi_{\text{iss}}$	0	$\frac{1}{2}$	0	0	0	$\frac{1}{2}$	0	0	0
$\phi_{\text{fss}}^+ \sigma_1(21) \sigma_1(34) \phi_{\text{iss}}$	0	0	0	$\frac{1}{2}$	0	0	0	$\frac{1}{2}$	0
$\phi_{\text{fss}}^+ \sigma_1(21) \sigma_2(34) \phi_{\text{iss}}$	0	0	0	$-\frac{1}{2}i$	0	0	0	$-\frac{1}{2}i$	0
$\phi_{\text{fss}}^+ \sigma_1(21) \sigma_3(34) \phi_{\text{iss}}$	0	0	0	0	$\frac{1}{2\sqrt{2}}$	0	0	0	$\frac{1}{\sqrt{2}}$
$\phi_{\text{fss}}^+ \sigma_2(21) \sigma_1(34) \phi_{\text{iss}}$	0	0	0	$-\frac{1}{2}i$	0	0	0	$-\frac{1}{2}i$	0
$\phi_{\text{fss}}^+ \sigma_2(21) \sigma_2(34) \phi_{\text{iss}}$	0	0	0	$-\frac{1}{2}$	0	0	0	$-\frac{1}{2}$	0
$\phi_{\text{fss}}^+ \sigma_2(21) \sigma_3(34) \phi_{\text{iss}}$	0	0	0	0	$-\frac{1}{2\sqrt{2}}i$	0	0	0	$-\frac{1}{\sqrt{2}}i$
$\phi_{\text{fss}}^+ \sigma_3(21) \sigma_1(34) \phi_{\text{iss}}$	$-\frac{1}{\sqrt{2}}$	0	0	0	$-\frac{1}{2\sqrt{2}}$	0	0	0	0
$\phi_{\text{fss}}^+ \sigma_3(21) \sigma_2(34) \phi_{\text{iss}}$	$\frac{1}{\sqrt{2}}i$	0	0	0	$\frac{1}{2\sqrt{2}}i$	0	0	0	0
$\phi_{\text{fss}}^+ \sigma_3(21) \sigma_3(34) \phi_{\text{iss}}$	0	$-\frac{1}{2}$	0	0	0	$-\frac{1}{2}$	0	0	0

Table 12: The same as Table 2 except for $S_D = 0$, $S_{Az} = 1$, and $S_A = S_B = S_C = 1$.

S_{Bz}	-1	-1	-1	0	0	0	1	1	1
S_{Cz}	-1	0	1	-1	0	1	-1	0	1
$\phi_{\text{fss}}^+ \phi_{\text{iss}}$	0	0	0	0	0	$-\frac{1}{2}$	0	$\frac{1}{2}$	0
$\phi_{\text{fss}}^+ \sigma_1(21) \phi_{\text{iss}}$	0	0	$-\frac{1}{\sqrt{2}}$	0	$\frac{1}{2\sqrt{2}}$	0	0	0	0
$\phi_{\text{fss}}^+ \sigma_2(21) \phi_{\text{iss}}$	0	0	$-\frac{1}{\sqrt{2}}i$	0	$\frac{1}{2\sqrt{2}}i$	0	0	0	0
$\phi_{\text{fss}}^+ \sigma_3(21) \phi_{\text{iss}}$	0	0	0	0	0	$-\frac{1}{2}$	0	$\frac{1}{2}$	0
$\phi_{\text{fss}}^+ \sigma_1(34) \phi_{\text{iss}}$	0	0	0	0	$-\frac{1}{2\sqrt{2}}$	0	0	0	$\frac{1}{\sqrt{2}}$
$\phi_{\text{fss}}^+ \sigma_2(34) \phi_{\text{iss}}$	0	0	0	0	$-\frac{1}{2\sqrt{2}}i$	0	0	0	$-\frac{1}{\sqrt{2}}i$
$\phi_{\text{fss}}^+ \sigma_3(34) \phi_{\text{iss}}$	0	0	0	0	0	$-\frac{1}{2}$	0	$-\frac{1}{2}$	0
$\phi_{\text{fss}}^+ \sigma_1(21) \sigma_1(34) \phi_{\text{iss}}$	0	$-\frac{1}{2}$	0	0	0	$\frac{1}{2}$	0	0	0
$\phi_{\text{fss}}^+ \sigma_1(21) \sigma_2(34) \phi_{\text{iss}}$	0	$-\frac{1}{2}i$	0	0	0	$-\frac{1}{2}i$	0	0	0
$\phi_{\text{fss}}^+ \sigma_1(21) \sigma_3(34) \phi_{\text{iss}}$	0	0	$-\frac{1}{\sqrt{2}}$	0	$-\frac{1}{2\sqrt{2}}$	0	0	0	0
$\phi_{\text{fss}}^+ \sigma_2(21) \sigma_1(34) \phi_{\text{iss}}$	0	$-\frac{1}{2}i$	0	0	0	$\frac{1}{2}i$	0	0	0
$\phi_{\text{fss}}^+ \sigma_2(21) \sigma_2(34) \phi_{\text{iss}}$	0	$\frac{1}{2}$	0	0	0	$\frac{1}{2}$	0	0	0
$\phi_{\text{fss}}^+ \sigma_2(21) \sigma_3(34) \phi_{\text{iss}}$	0	0	$-\frac{1}{\sqrt{2}}i$	0	$-\frac{1}{2\sqrt{2}}i$	0	0	0	0
$\phi_{\text{fss}}^+ \sigma_3(21) \sigma_1(34) \phi_{\text{iss}}$	0	0	0	0	$-\frac{1}{2\sqrt{2}}$	0	0	0	$\frac{1}{\sqrt{2}}$
$\phi_{\text{fss}}^+ \sigma_3(21) \sigma_2(34) \phi_{\text{iss}}$	0	0	0	0	$-\frac{1}{2\sqrt{2}}i$	0	0	0	$-\frac{1}{\sqrt{2}}i$
$\phi_{\text{fss}}^+ \sigma_3(21) \sigma_3(34) \phi_{\text{iss}}$	0	0	0	0	0	$-\frac{1}{2}$	0	$-\frac{1}{2}$	0

Table 13: The same as Table 2 except for $S_D = 0$, $S_{Az} = 0$, and $S_A = S_B = S_C = 1$.

S_{Bz}	-1	-1	-1	0	0	0	1	1	1
S_{Cz}	-1	0	1	-1	0	1	-1	0	1
$\phi_{\text{fss}}^+ \phi_{\text{iss}}$	0	0	$-\frac{1}{2}$	0	0	0	$\frac{1}{2}$	0	0
$\phi_{\text{fss}}^+ \sigma_1(21) \phi_{\text{iss}}$	0	$-\frac{1}{2\sqrt{2}}$	0	$\frac{1}{2\sqrt{2}}$	0	$-\frac{1}{2\sqrt{2}}$	0	$\frac{1}{2\sqrt{2}}$	0
$\phi_{\text{fss}}^+ \sigma_2(21) \phi_{\text{iss}}$	0	$-\frac{1}{2\sqrt{2}}i$	0	$\frac{1}{2\sqrt{2}}i$	0	$\frac{1}{2\sqrt{2}}i$	0	$-\frac{1}{2\sqrt{2}}i$	0
$\phi_{\text{fss}}^+ \sigma_3(21) \phi_{\text{iss}}$	0	0	$\frac{1}{2}$	0	$-\frac{1}{2}$	0	$\frac{1}{2}$	0	0
$\phi_{\text{fss}}^+ \sigma_1(34) \phi_{\text{iss}}$	0	$-\frac{1}{2\sqrt{2}}$	0	$-\frac{1}{2\sqrt{2}}$	0	$\frac{1}{2\sqrt{2}}$	0	$\frac{1}{2\sqrt{2}}$	0
$\phi_{\text{fss}}^+ \sigma_2(34) \phi_{\text{iss}}$	0	$-\frac{1}{2\sqrt{2}}i$	0	$-\frac{1}{2\sqrt{2}}i$	0	$-\frac{1}{2\sqrt{2}}i$	0	$-\frac{1}{2\sqrt{2}}i$	0
$\phi_{\text{fss}}^+ \sigma_3(34) \phi_{\text{iss}}$	0	0	$-\frac{1}{2}$	0	$-\frac{1}{2}$	0	$-\frac{1}{2}$	0	0
$\phi_{\text{fss}}^+ \sigma_1(21) \sigma_1(34) \phi_{\text{iss}}$	$-\frac{1}{2}$	0	0	0	0	0	0	0	$\frac{1}{2}$
$\phi_{\text{fss}}^+ \sigma_1(21) \sigma_2(34) \phi_{\text{iss}}$	$-\frac{1}{2}i$	0	0	0	$-\frac{1}{2}i$	0	0	0	$-\frac{1}{2}i$
$\phi_{\text{fss}}^+ \sigma_1(21) \sigma_3(34) \phi_{\text{iss}}$	0	$-\frac{1}{2\sqrt{2}}$	0	$-\frac{1}{2\sqrt{2}}$	0	$-\frac{1}{2\sqrt{2}}$	0	$-\frac{1}{2\sqrt{2}}$	0
$\phi_{\text{fss}}^+ \sigma_2(21) \sigma_1(34) \phi_{\text{iss}}$	$-\frac{1}{2}i$	0	0	0	$\frac{1}{2}i$	0	0	0	$-\frac{1}{2}i$
$\phi_{\text{fss}}^+ \sigma_2(21) \sigma_2(34) \phi_{\text{iss}}$	$\frac{1}{2}$	0	0	0	0	0	0	0	$-\frac{1}{2}$
$\phi_{\text{fss}}^+ \sigma_2(21) \sigma_3(34) \phi_{\text{iss}}$	0	$-\frac{1}{2\sqrt{2}}i$	0	$-\frac{1}{2\sqrt{2}}i$	0	$\frac{1}{2\sqrt{2}}i$	0	$\frac{1}{2\sqrt{2}}i$	0
$\phi_{\text{fss}}^+ \sigma_3(21) \sigma_1(34) \phi_{\text{iss}}$	0	$\frac{1}{2\sqrt{2}}$	0	$-\frac{1}{2\sqrt{2}}$	0	$-\frac{1}{2\sqrt{2}}$	0	$\frac{1}{2\sqrt{2}}$	0
$\phi_{\text{fss}}^+ \sigma_3(21) \sigma_2(34) \phi_{\text{iss}}$	0	$\frac{1}{2\sqrt{2}}i$	0	$-\frac{1}{2\sqrt{2}}i$	0	$\frac{1}{2\sqrt{2}}i$	0	$-\frac{1}{2\sqrt{2}}i$	0
$\phi_{\text{fss}}^+ \sigma_3(21) \sigma_3(34) \phi_{\text{iss}}$	0	0	$\frac{1}{2}$	0	0	0	$-\frac{1}{2}$	0	0

Table 14: The same as Table 2 except for $S_D = 0$, $S_{Az} = -1$, and $S_A = S_B = S_C = 1$.

S_{Bz}	-1	-1	-1	0	0	0	1	1	1
S_{Cz}	-1	0	1	-1	0	1	-1	0	1
$\phi_{\text{fss}}^+ \phi_{\text{iss}}$	0	$-\frac{1}{2}$	0	$\frac{1}{2}$	0	0	0	0	0
$\phi_{\text{fss}}^+ \sigma_1(21) \phi_{\text{iss}}$	0	0	0	0	$-\frac{1}{2\sqrt{2}}$	0	$\frac{1}{\sqrt{2}}$	0	0
$\phi_{\text{fss}}^+ \sigma_2(21) \phi_{\text{iss}}$	0	0	0	0	$\frac{1}{2\sqrt{2}}i$	0	$-\frac{1}{\sqrt{2}}i$	0	0
$\phi_{\text{fss}}^+ \sigma_3(21) \phi_{\text{iss}}$	0	$\frac{1}{2}$	0	$-\frac{1}{2}$	0	0	0	0	0
$\phi_{\text{fss}}^+ \sigma_1(34) \phi_{\text{iss}}$	$-\frac{1}{\sqrt{2}}$	0	0	0	$\frac{1}{2\sqrt{2}}$	0	0	0	0
$\phi_{\text{fss}}^+ \sigma_2(34) \phi_{\text{iss}}$	$-\frac{1}{\sqrt{2}}i$	0	0	0	$-\frac{1}{2\sqrt{2}}i$	0	0	0	0
$\phi_{\text{fss}}^+ \sigma_3(34) \phi_{\text{iss}}$	0	$-\frac{1}{2}$	0	$-\frac{1}{2}$	0	0	0	0	0
$\phi_{\text{fss}}^+ \sigma_1(21) \sigma_1(34) \phi_{\text{iss}}$	0	0	0	$-\frac{1}{2}$	0	0	0	$\frac{1}{2}$	0
$\phi_{\text{fss}}^+ \sigma_1(21) \sigma_2(34) \phi_{\text{iss}}$	0	0	0	$-\frac{1}{2}i$	0	0	0	$-\frac{1}{2}i$	0
$\phi_{\text{fss}}^+ \sigma_1(21) \sigma_3(34) \phi_{\text{iss}}$	0	0	0	0	$-\frac{1}{2\sqrt{2}}$	0	$-\frac{1}{\sqrt{2}}$	0	0
$\phi_{\text{fss}}^+ \sigma_2(21) \sigma_1(34) \phi_{\text{iss}}$	0	0	0	$\frac{1}{2}i$	0	0	0	$-\frac{1}{2}i$	0
$\phi_{\text{fss}}^+ \sigma_2(21) \sigma_2(34) \phi_{\text{iss}}$	0	0	0	$-\frac{1}{2}$	0	0	0	$-\frac{1}{2}$	0
$\phi_{\text{fss}}^+ \sigma_2(21) \sigma_3(34) \phi_{\text{iss}}$	0	0	0	0	$\frac{1}{2\sqrt{2}}i$	0	$\frac{1}{\sqrt{2}}i$	0	0
$\phi_{\text{fss}}^+ \sigma_3(21) \sigma_1(34) \phi_{\text{iss}}$	$\frac{1}{\sqrt{2}}$	0	0	0	$-\frac{1}{2\sqrt{2}}$	0	0	0	0
$\phi_{\text{fss}}^+ \sigma_3(21) \sigma_2(34) \phi_{\text{iss}}$	$\frac{1}{\sqrt{2}}i$	0	0	0	$\frac{1}{2\sqrt{2}}i$	0	0	0	0
$\phi_{\text{fss}}^+ \sigma_3(21) \sigma_3(34) \phi_{\text{iss}}$	0	$\frac{1}{2}$	0	$\frac{1}{2}$	0	0	0	0	0

Table 15: Flavor matrix elements.

Channel	$\mathcal{M}_{aq_1\bar{q}_2f}$	$\mathcal{M}_{a\bar{q}_1q_2f}$
$I = 1 \ \pi\pi \rightarrow \rho\rho$	1	1
$I = 0 \ \pi\pi \rightarrow \rho\rho$	$\frac{3}{2}$	$\frac{3}{2}$
$I = 1 \ K\bar{K} \rightarrow K^*\bar{K}^*$	0	1
$I = 0 \ K\bar{K} \rightarrow K^*\bar{K}^*$	2	1
$I = 1 \ K\bar{K}^* \rightarrow K^*\bar{K}^*$	0	1
$I = 0 \ K\bar{K}^* \rightarrow K^*\bar{K}^*$	2	1
$I = 1 \ K^*\bar{K} \rightarrow K^*\bar{K}^*$	0	1
$I = 0 \ K^*\bar{K} \rightarrow K^*\bar{K}^*$	2	1
$I = 1 \ \pi\pi \rightarrow K\bar{K}$	0	-1
$I = 0 \ \pi\pi \rightarrow K\bar{K}$	0	$-\frac{\sqrt{6}}{2}$
$I = 1 \ \pi\rho \rightarrow K\bar{K}^*$	0	-1
$I = 0 \ \pi\rho \rightarrow K\bar{K}^*$	0	$-\frac{\sqrt{6}}{2}$
$I = 1 \ \pi\rho \rightarrow K^*\bar{K}$	0	-1
$I = 0 \ \pi\rho \rightarrow K^*\bar{K}$	0	$-\frac{\sqrt{6}}{2}$
$I = 1 \ K\bar{K} \rightarrow \rho\rho$	0	-1
$I = 0 \ K\bar{K} \rightarrow \rho\rho$	0	$-\frac{\sqrt{6}}{2}$

Table 16: Values of the parameters. a_1 and a_2 are in units of millibarns; b_1 , b_2 , d_0 , and $\sqrt{s_z}$ are in units of GeV; c_1 and c_2 are dimensionless.

Reactions	T/T_c	a_1	b_1	c_1	a_2	b_2	c_2	d_0	$\sqrt{s_z}$
$I = 1 \pi\pi \rightarrow \rho\rho$	0	0.19	1.4	4.2	1.08	0.35	0.67	0.35	7.76
	0.65	0.11	1.3	6.8	0.2	0.27	0.54	0.25	5.05
	0.75	0.042	1.46	10.55	0.086	0.34	0.51	0.25	4.57
	0.85	0.015	1.69	12.6	0.027	0.35	0.48	0.3	4.13
	0.9	0.0085	1.84	9.13	0.0166	0.3	0.45	0.2	4.01
	0.95	0.0089	1.9	6.9	0.022	0.29	0.48	0.25	3.87
$I = 1 K\bar{K} \rightarrow K^*\bar{K}^*$	0	0.95	0.13	0.53	0.17	0.48	1.07	0.15	3.81
	0.65	0.6	0.142	0.52	0.133	0.79	4.54	0.15	3.28
	0.75	0.049	1.02	9.24	0.349	0.2	0.49	0.2	3.19
	0.85	0.109	0.145	0.47	0.068	1.12	6.27	0.125	3.19
	0.9	0.121	0.069	0.45	0.082	1.28	1.39	0.071	3.15
	0.95	0.181	0.052	0.43	0.158	5.89	0.5	0.0418	3.03
$I = 0 K\bar{K} \rightarrow K^*\bar{K}^*$	0	1.74	1.3	0.42	4.71	0.186	0.55	0.2	10.36
	0.65	1.45	0.54	0.99	1.87	0.09	0.51	0.15	9.22
	0.75	1.42	0.155	0.51	0.47	0.98	4.04	0.175	8.4
	0.85	0.2	0.83	2.74	0.42	0.1	0.49	0.1126	4.73
	0.9	0.38	0.051	0.61	0.27	0.24	0.31	0.0418	3.3
	0.95	0.75	0.026	0.55	0.51	0.132	0.33	0.025	2.77

Table 17: The same as Table 16, but for three other reactions.

Reactions	T/T_c	a_1	b_1	c_1	a_2	b_2	c_2	d_0	$\sqrt{s_z}$
$I = 1 \ K \bar{K}^* \rightarrow K^* \bar{K}^*$	0	1.4	0.08	0.8	2.19	0.13	0.45	0.1	3.52
	0.65	0.36	0.87	4.82	1.08	0.11	0.49	0.1	3.33
	0.75	0.6	0.11	0.46	0.29	1.01	6.85	0.075	3.28
	0.85	0.33	0.056	0.43	0.173	1.35	1.56	0.0418	3.18
	0.9	0.48	0.041	0.4	0.22	2.69	0.9	0.025	3.16
	0.95	0.61	0.036	0.36	0.29	3.67	0.92	0.025	3.02
$I = 0 \ K \bar{K}^* \rightarrow K^* \bar{K}^*$	0	1.4	0.9	2.65	8.9	0.1	0.5	0.1	7.96
	0.65	0.35	0.05	0.72	2.5	0.13	0.45	0.1	5.6
	0.75	0.1	0.61	4.58	1.64	0.1	0.47	0.1	4.15
	0.85	1.08	0.06	0.44	0.09	0.5	2.15	0.05	2.46
	0.9	0.79	0.15	1.49	2.04	0.019	0.47	0.025	1.99
	0.95	0.78	0.18	0.63	3.6	0.017	0.41	0.0126	1.62
$I = 1 \ \pi\pi \rightarrow K \bar{K}$	0	0.02	0.068	0.82	0.088	0.29	2.83	0.3	2.26
	0.65	0.03	0.06	0.8	0.13	0.28	2.76	0.28	2.1
	0.75	0.04	0.11	0.8	0.09	0.3	3.5	0.25	9.1
	0.85	0.064	0.3	3.89	0.031	0.11	0.76	0.219	7.26
	0.9	0.021	0.092	0.74	0.051	0.3	3.72	0.28	6.32
	0.95	0.0136	0.038	0.75	0.0407	0.29	2.83	0.3	6.17

Table 18: The same as Table 16, but for three other reactions.

Reactions	T/T_c	a_1	b_1	c_1	a_2	b_2	c_2	d_0	$\sqrt{s_z}$
$I = 1 \pi \rho \rightarrow K \bar{K}^*$	0	0.1	0.96	0.71	0.66	0.16	0.64	0.175	4.08
	0.65	0.048	0.62	0.98	0.17	0.12	0.52	0.125	3.81
	0.75	0.02	0.43	0.38	0.064	0.16	0.57	0.15	3.69
	0.85	0.004	0.54	0.27	0.027	0.25	0.84	0.25	3.36
	0.9	0.0076	0.33	0.38	0.024	0.25	0.92	0.25	3.15
	0.95	0.008	0.22	1.21	0.053	0.22	0.49	0.2	3.05
$I = 1 \pi \rho \rightarrow K^* \bar{K}$	0	0.37	0.17	1.34	0.32	0.36	0.54	0.25	4.67
	0.65	0.034	0.12	1.01	0.065	0.35	0.47	0.2	4.05
	0.75	0.015	0.09	0.5	0.024	0.5	0.71	0.2	3.86
	0.85	0.0074	0.21	0.49	0.004	1.21	8.98	0.2	3.41
	0.9	0.0045	0.19	0.48	0.003	1.29	6.6	0.2	3.25
	0.95	0.0062	0.162	0.48	0.0038	1.39	4.95	0.15	3.18
$I = 1 K \bar{K} \rightarrow \rho \rho$	0	0.77	0.08	0.53	0.49	0.64	1.29	0.11	5.99
	0.65	0.175	0.133	0.49	0.108	1.27	3.6	0.13	5.52
	0.75	0.112	0.065	0.44	0.056	1.08	1.5	0.05	5.28
	0.85	0.021	0.116	0.45	0.0173	1.55	3.44	0.1	4.83
	0.9	0.0117	0.15	0.47	0.0122	1.65	2.89	0.15	4.77
	0.95	0.0068	0.08	0.47	0.0118	1.2	0.79	0.3	4.7